NASA Reference Publication 1239

November 1990

Failure Behavior of Generic Metallic and Composite Aircraft Structural Components Under Crash Loads

Huey D. Carden
and Martha P. Robinson

NASA

NASA Reference Publication 1239

1990

Failure Behavior of Generic Metallic and Composite Aircraft Structural Components Under Crash Loads

Huey D. Carden
and Martha P. Robinson
Langley Research Center
Hampton, Virginia

NASA
National Aeronautics and Space Administration
Office of Management
Scientific and Technical Information Division

Summary

Failure behavior results are presented from crash dynamics research using concepts of aircraft elements and substructure not necessarily designed or optimized for energy absorption or crash loading considerations. To achieve desired new designs incorporating improved energy absorption capabilities often requires an understanding of how more conventional designs behave under crash loadings. The experimental and analytical data presented indicate some general trends in the failure behavior of a class of composite structures including individual fuselage frames, skeleton subfloors with stringers and floor beams without skin covering, and subfloors with skin added to the frame-stringer arrangement. Although the behavior is complex, a strong similarity in the static and dynamic failure behavior of these structures is illustrated through photographs of the experimental results and through analytical data of generic composite structural models. The similarity in behavior gives designers and dynamists much information on the crash behavior of these structures and can guide designs for improving the energy absorption and crash behavior of such structures.

Introduction

The NASA Langley Research Center has been involved in crash dynamics research since the early 1970's. For nearly 10 years the emphasis of the research was on metal aircraft structures during the General Aviation Crash Dynamics Program (refs. 1 to 13) and a transport aircraft program, the Controlled Impact Demonstration (CID), which culminated in the remotely piloted crash test of a Boeing 720 aircraft in 1984 (refs. 14 to 16). Since the transport work, the emphasis has been on composite structures, with efforts directed at developing a data base for understanding the behavior, responses, failure mechanisms, and general loads associated with composite material systems under crash loadings (see fig. 1). Considerable work has been conducted to determine the energy absorption characteristics of composites (refs. 17 to 20), and the research indicates that composites can absorb as much energy as, if not considerably more than, comparable aluminum structures. However, because of the brittle nature of composites, attention must be given to designs that will take advantage of the good energy-absorbing properties in crash situations while providing the desired structural integrity. To achieve desired new designs requires an understanding of the behavior of conventional designs under crash loadings.

The purpose of this paper is to present data on the observed failure behavior from research conducted using concepts of aircraft substructure not necessarily designed (or optimized) for energy absorption or crash loading considerations. The experimental and analytical data indicate some general trends in the failure behavior of a class of composite structures that includes individual fuselage frames, skeleton subfloors with stringers and floor beams but without skin covering, and subfloors with skin over the frame-stringer arrangement. Although the behavior is complex, a strong similarity in the static and dynamic failure behavior of these structures is illustrated through photographs of the damaged structures and through analytical data of generic composite structural models. The similarity in behavior gives designers and dynamists much insight into the crash behavior of these structures and can be used to great advantage in improving the energy absorption and crash behavior of such structures.

Impact Dynamics Research Facility

Much of the information presented in this report is the result of a research program to investigate the impact response of metal and composite aircraft components conducted at the Langley Impact Dynamics Research Facility (IDRF). The IDRF (shown in fig. 2) is the former Lunar Landing Facility, which was used to train astronauts for moon landings. The facility is 230 ft high and 400 ft long. In the early 1970's, the structure was converted for crash testing full-scale general aviation aircraft. Reference 21 provides complete details of the facility and test techniques for full-scale aircraft testing. Additionally, a 70-ft-high Vertical Drop Test Apparatus used for full-scale aircraft section, component, and/or seat testing is shown in figure 3. Static testing machines and other apparatus are also available at the facility for metal and composite aircraft structural testing.

Analysis

To gain an understanding of the fundamental physical behavior of complex structures, experimental research with structures under crash loadings is generally accompanied by analytical prediction/correlation studies whenever feasible. Thus, various finite element codes that have capabilities for handling the dynamic, large displacement, nonlinear response of metal and composite structures are used as tools in the research efforts.

The analytical results presented here were generated with a nonlinear finite element computer code called DYCAST (DYnamic Crash Analysis of STructures (ref. 22) developed by Grumman Aerospace

Corporation with principal support from NASA and the Federal Aviation Administration. The basic element library consists of (1) stringers with axial stiffness only; (2) beam elements with 12 fixed cross-sectional shapes typical of aircraft structures with axial and torsional stiffnesses, and two bending and two shear stiffnesses; (3) isotropic and orthotropic membrane skin triangles with membrane stiffnesses; (4) isotropic plate-bending triangles with membrane and out-of-plane bending stiffnesses; and (5) nonlinear translational or rotational spring elements that provide stiffness with user-specified force-displacement or moment-rotation tables (piecewise linear). The spring element can be either elastic or dissipative. The springs are useful to model crush behavior of components for which experimental or analytical data are available and/or whose behavior may be too complex or time consuming to model otherwise. An effort is underway to add curved composite beam, composite plate, and curved shell elements to the DYCAST element library.

Other analysis codes such as the NIKE and DYNA codes developed at the Lawrence Livermore National Laboratory, Livermore, California, and the MacNeal-Schwendler Corporation MSC/DYNA version of the DYNA code are used on selected problems in the composite impact research. Additionally, through university grants other approaches to efficient analysis techniques are being explored for composite applications (see refs. 23 to 25). However, as stated earlier, the analytical results of this paper have been generated with the DYCAST code.

Test Specimens and Description

Full-Scale Aircraft

Metal aircraft structures. Langley Research Center conducted three vertical drop tests of 12-foot-long fuselage sections cut from an out-of-service Boeing 707 aircraft to support transport research efforts. Selected data on the crash behavior of the transport aircraft sections (refs. 26 and 27) are included in this paper to demonstrate important similarities in the behavior of both metal and composite fuselage structures. The fuselage sections were drop tested at 20 ft/sec to measure structural, seat, and occupant responses to vertical crash loads and to provide data for nonlinear finite element modeling. The two sections of interest were cut forward and aft of the wing location. A photograph of the forward section suspended in the Vertical Drop Test Apparatus at the IDRF is shown in figure 4. The aft section contained seats, anthropomorphic dummies, a data acquisition system pallet, a power pallet, and camera batteries. This test served two purposes: (1) to test structural, seat, and occupant responses and (2) to test the data acquisition system and instrumentation to be used in the remotely piloted full-scale transport crash test on the Controlled Impact Demonstration (CID). The reader should refer to the particular reports (refs. 14, 15, 16, 26, and 27) for more complete descriptions of the test articles since such information is not repeated in this report.

Composite aircraft structures. The IDRF at Langley Research Center supported the Army Advanced Composite Aircraft Program (ACAP) by conducting the tests of two specially designed full-scale composite aircraft structures (fig. 5). (See refs. 28 and 29.) The sensitivity of the data preclude their inclusion in this paper. However, two full-scale, composite general aviation aircraft structures; two complete wing sets; and landing gears have been obtained for testing at the IDRF to add to the data base being generated. One of the composite aircraft fuselage specimens is shown in figure 6.

Composite Aircraft Components

Composite fuselage panel. As part of the Aircraft Energy Efficiency (ACEE) Program, the static and dynamic behavior of the lower fuselage composite structure was evaluated (ref. 30). Development tests were performed on the composite structures to verify that the composite structure, designed to the same operating load as the metal design, could have at least the same energy absorption capability as aluminum structure. A photograph of the composite fuselage panel in the static testing machine is shown in figure 7. Load-displacement and failure behavior determined for the corrugated frame/skin test panel are included herein for comparison with other composite structures. The frame/skin specimen had a 117.5-in. radius (to outside skin), was 60 in. long by 30 in. wide, and had two corrugated frames on 20-in. spacing. Fabrication techniques and more complete details of the frame/skin panel are given in reference 30.

Single composite frames. Various cross-sectional shapes for fuselage frames are used in metal aircraft and are often proposed for composite structures. Figure 8 shows sketches and photographs of four of the more common geometries, Z-, I-, J-, and C-cross-sectional shapes, of which circular frames were fabricated for testing to add information to the composite structures data base. To add out-of-plane stability to the frame concepts (with the exception of the Z-section frames), 2.25- or 3.5-in-wide skin material was added, which enhanced the ease of testing of both symmetrical and nonsymmetrical sections. The

Table I. Composite Frame Section Lay-Ups

Fuselage frame label	Serial number	Configuration	Lay-up	Weight, kg
FR004I	1	I-section	$(\pm 45/0/90)_s$	1.443
FR005I	1	I-section	$(\pm 45/0/90)_{2s}$	1.996
FR004J	2	J-section	$(\pm 45/0/90)_{2s}$	1.853
FR005C	1	C-section	$(\pm 45/0/90)_{2s}$	1.229
FR005C	2	C-section	$(\pm 45/0/90)_{2s}$	1.229

0.08-in-thick, 16-ply skin with a $[\pm 45/0/90]_{2s}$ lay-up was cocured with the 6-ft-diameter frames, which have the lay-ups as indicated in table I. The frames were constructed in two heights, 1.25 in. and 0.75 in., to investigate the effect of frame height on behavior and responses.

One of the first geometries to be studied under static and dynamic loadings was the Z-cross section. A photograph of Z-cross section fuselage frames used in the initial studies of the behavior of composite structural elements under impact loads is shown in figure 8(c). A Z-frame suspended in the drop apparatus prior to testing is shown in figure 9. The apparatus was constructed with guide rails, a rear metal backstop, and a front Plexiglass sheet. During free-fall the specimen was guided, and the front and rear backstops prevented appreciable (but not all) out-of-plane bending or twisting during impact and allowed photographic or motion picture coverage through the front Plexiglas plate. The 6-ft-diameter frames were constructed using a quasi-isotropic lay-up of 280-5HA/3502, a five-harness, satin weave graphite fabric composite material. The Z-cross section of the frame was 3 in. high with a total width of 2.25 in. and a thickness of about 0.08 in. Initial tests were with 360° frames made from four 90° segments joined with splice plates as shown in figure 8(c). Additional tests were conducted with half-frames since the top half of the complete frames were undamaged in the tests.

The approach of studying simple structural elements and then moving to combinations of these elements in more complex substructures has been taken in the development of a data base on the dynamic response and behavior of composite aircraft structures. The approach parallels the one used during the general aviation and transport aircraft programs. Consequently, three composite subfloor structures were fabricated following the initial investigation of the Z-frames discussed above.

Composite subfloors. A photograph of composite subfloor specimens constructed with three of the single Z-section frames similar to those that were studied earlier is shown in figure 10. Pultruded J-stringers connected the three frames through metal clips and secondary bonding methods. Aluminum floor beams tied the upper end of the frames together to form the lower half of the subfloor. Notches in the frames allowed the stringers to pass through the frames. Two subfloors without skin were fabricated. A third specimen had a ±45° lay-up skin bonded and riveted to the frames to form the lower fuselage structure.

Results and Discussion

Experimental and analytical results from the studies of full-scale aircraft structures, composite fuselage panels, frames, and subfloors under static and/or dynamic loadings are presented in figures 11 to 24. The photographs emphasize the failure behavior of the composite and metal components, which show a strong similarity in their behavior. The behavior is thought to be an important consideration in the design of new structures for improving the energy absorption and crash behavior of these components and structural elements.

Full-Scale Metal Aircraft Structures

Experimental and analytical results from studies with full-scale transport aircraft sections (from refs. 26 and 27) are presented in figure 11.

Dynamic tests. The resulting structural damage to the transport aircraft structures from the 20 ft/sec vertical drop tests is shown in figures 11(a) and (b). The damage to the transport sections was confined to the lower fuselage below the floor. All seven frames ruptured near the bottom impact point. Plastic hinges formed in each frame along both sides of the fuselage approximately 50° up the circumference from the bottom contact point (see fig. 11(c)).

The crushing of the lower fuselage was approximately 22–23 in. at the front end and 18–19 in. at the rear for the section forward of the wing (fig. 11(a)). For the aft section (fig. 11(b)), the crushing was about 14 in. at front and 18 in. at the rear. Although the aircraft structures are metal and the failures discussed above involve plastic deformations with some tearing of the metal rather than brittle fracturing, the general observed failure pattern and failure locations for the transport fuselage sections will be shown to be quite similar to those of the composite frames and subfloors discussed later.

Analytical studies. A DYCAST model of the forward section of the transport fuselage was generated to model the floor, two seats with lumped mass occupants, and the fuselage structure to determine if such a model could predict the response of the complete section with fidelity. The finite element model is shown in figure 12. Stiff ground springs simulated the concrete impact surface. Each frame of the fuselage below the floor was modeled with eight beam elements, and the floor and seat rails were also modeled with appropriate beam elements. The fuselage structure above the floor (not expected to fail) was modeled in less detail. Two triple-occupant seats were modeled with four lumped masses connected by horizontal stringers supported by four nonlinear springs for the vertical legs. The mass of three occupants was distributed on a 2:1 ratio, with the inboard seat legs supporting two occupants and the outboard legs supporting one occupant because of asymmetry of the seat pan with respect to the legs.

A comparison of the analytical predictions of the two-frame model and full-section experimental responses is shown in figure 13. As shown in the figure, the correlation of vertical displacements and wall/floor and dummy pelvis accelerations are considered good. Figure 14 shows the deformation pattern of the two frame model. As may be noted, the overall impression from the analytical model deformation pattern is quite similar to the behavior seen in the experiment with the full-section shown in figure 11. Thus, the full-section behavior was basically contained in the two-frame model.

Full-Scale Composite Aircraft

Other than the two drop tests of the composite helicopters conducted for the Army (refs. 28 and 29), no full-scale composite aircraft have been tested yet at the Langley Research Center as part of the composite impact dynamics research. However, as mentioned previously, two full-scale composite general aviation aircraft structures, two complete wing sets, and landing gears are available for testing.

In the following sections, the composite impact dynamics studies have taken the building block approach of using a sequence of tests and analyses that begins with "simpler" elements and moves to more "complicated" components or substructures. As mentioned earlier, this approach was used in the general aviation (GA) and transport programs, although the GA data base was being concurrently developed through full-scale testing. Full-scale crash tests using currently available composite aircraft specimens and/or other full-scale composite structures are part of the ongoing research program.

Composite Fuselage Panel Study

Figure 15 shows the failure behavior and the static load displacement data for the corrugated frame/skin specimen from the ACEE program. Figure 15(a) indicates that the load increased linearly to failure, whereupon the load dropped substantially as a result of fracturing of the corrugated frames at locations (0° and 6.2°) near the center (loading region) of the panel. Additionally, some delamination of the frame caps occurred during the loading. Once the panel was removed from the test apparatus, the snap-through condition of the skin was reversed, as may be noted in figure 15(b). The fractures of the corrugated frame and some delamination of the frame caps, mentioned above, are the only visible damage to the structure.

Composite Single Frame Studies

Static tests. Results from the static test of a composite semicircular frame (ref. 31) with a Z-cross section are presented in figure 16. A photograph of the static test apparatus in figure 16(a) shows that the splice plate was at the load point. Consequently, the frame failed just outside the doubler splice plate area by a complete fracture across the Z-section. Load deflection data and the failure locations are shown in figure 16(b). The load deflection data show a saw-toothed behavior of loading and unloading. The load increased linearly until initial failure, then fell off to under 600 lb force. Subsequent loading of the frame after initial failure is at a new, reduced stiffness. Second and third fractures occurred up the side again at approximately 54° and 58° under continued loading, as may be noted in the sketch at the right of figure 16(b). Photographic data in figure 16(c) show that the initial failure was induced by a local buckling of the frame, which occurred at about 18° from the bottom loading point outside the splice plate area.

Static analytical studies. To demonstrate analytically the apparent behavior of the frames under

load (exclusive of the local buckling that actually initiated the failure in the static tests), two DYCAST finite element models were generated. For ease of analysis, a typical I-section was modeled from the specimens described in the section "Single Composite Frames." Figure 17(a) shows the load displacement plots for the two models. In case I, the frame was loaded at the top and a simulated ground plane (ground contact springs) resisted the vertical movement of the frame during load application. A half frame was modeled using 34 I-section beam elements with boundary conditions imposed at the bottom node to account for the symmetrical situation. The top node was constrained to allow only vertical displacement, thus simulating the effect of a very stiff floor across the frame diameter. The static load was slowly increased until the input failure strain for the material (0.0086) was exceeded at the point of loading, and failure was indicated.

A second DYCAST model, case II, was run wherein the bottom point of the frame was modeled with two short skin segments to represent the different condition of the structure following the initial failure of the frame. This condition will be discussed further relative to the composite subfloor test with the skinned subfloor specimen. Essentially, the frame load increases along the curve of case I to the point of initial failure at the bottom of the frame. After the frame fractures, the structure has changed to one considerably weakened—down to the bending stiffness of the skin alone at that location. The load then drops to the lower curve, case II, which represents the stiffness of the section, which has been weakened on the bottom end of the frame. The load continues along the curve of case II until secondary failures occur at other locations on the frame circumference.

An examination of the case I normalized distribution of the bending moment on the frame, shown in figure 17(b), provides a better understanding of the failure behavior. Maximum moment is indicated (just prior to failure) to be at the 0° location, with secondary maximums between ±50°–60° from the bottom contact area. The locations correlate well with the failure locations in the experiment with the Z-frame. As may be recalled, the composite corrugated frame/skin fuselage panel specimens from the ACEE Program also showed failure location near the 0° load region, although the panel represented only the extreme bottom segment of the fuselage with clamped boundaries on the curvature ends of the specimen. The maximum moment on the frame/skin segment was at the 0° or loading region of the panel, similar to the distributions for the frame models discussed above.

The normalized bending moment distribution on the broken frame for case II is presented in figure 17(c). As may be noted, the distribution is quite similar to the case I initial model results in figure 17(b). The failure locations are at the maximum bending moment locations predicted, about ±45°, which are somewhat lower than the maximum bending moment locations shown in the initial model of the unbroken frame. The agreement between the behavior predicted by the two models and the experimental results, however, is still considered good.

To show the effect of the frame diameter on the moment distribution, the diameter of the frame model was increased by a factor of two (to 75 in.). The normalized moment distribution was found to be essentially identical to the smaller diameter frame results of figures 17(b) and 17(c). Moment distribution in terms of geometry and load for a point-loaded ring (ref. 32) shows that the maximum moment will occur at the same angle for different diameters. This suggests that the larger transport sections should probably have failure locations identical to the smaller diameter frames.

Additionally, to show the effect of floor location (simulated by constraints in the analytical model) on the moment distribution of the frame, the constraints and load application points were moved from the diameter to positions that resulted in 120°, 90°, and 60° frame segments below the floor. The bending moment distributions for these models under the same applied load are given in figure 17(d). The results indicate that the distribution is still similar to the full 180° frame distribution, but the location of the maximum moment away from the contact region falls below those locations on the half-circle model. Also, the maximum moment for the same applied load is less than that of the full half-circle model. Since the arc length of the frame decreases with the lower floor locations, the moment arm of the applied load is also decreased, thus resulting in reduced moments for a given load. However, the magnitude of the maximum moment at the contact region was still approximately 2.1 greater than the magnitude of the other circumferential maximums prior to any failure.

Furthermore, a comparison of the analytical cases (fig. 17(a)) with the actual static load deflection of the Z-section (fig. 16(b)) indicates very similar load deflection behavior patterns, as discussed above. Although the Z-frame had no skin, if the ends jam together (as they did in several cases), the boundary is effectively between the skin-stiffened case and a guided boundary. Thus, the predicted failure in the simple beam-frame model at about 50°–55° agrees

well with the 54° and 58° failure locations in the experiment with the Z-section frame.

Without a priori knowledge of the manner of the failure discussed above, the initial formulation of a finite element model would probably not incorporate the necessary failure behavior for the frames. However, knowing the pattern of behavior can enable the analysts to formulate adequate finite element models to predict dynamic responses, including failure and crash loadings. Additionally, such information is important to designers of new structures so that they can design for impact loads on such structural elements of an aircraft fuselage.

Dynamic tests. Information from reference 33 on the dynamic studies of the response of composite frames is shown in figure 18. As shown in figure 18(a), the splice plates joining the segments of the frame are 45° up the circumference from the point of impact. As noted in figure 18(b), complete failures (fractures) of the Z-section frames occurred at the bottom and approximately 60° from the bottom. It appears that the presence of the splice plates moved the top failure points up a few degrees (to about the 60° locations).

Dynamic analytical studies. Experimental and analytical model results for the composite Z-frame subjected to a 20 ft/sec impact are shown in figure 19. The results show the first 15 msec of the experimental acceleration for the floor and two analytical model predictions. In one analysis model, the in-plane deformations were constrained to the plane of the frame, whereas in the other the frame was free to twist and bend out of plane. As shown in the figure, the agreement between the "free" model and the experiment is good for the initial peak load. Later the agreement is not as good because the backstop and clear fences in the experiment, which were not modeled, began to provide support to the twisting and bending frame. The in-plane model results are about 60 percent higher than the experiment and "free" model results. The results emphasize the importance of modeling the "exact" experimental boundary conditions to understand the dynamic (and static) behavior of structures under crash-type loadings. Unfortunately, mixed boundary conditions often exist or occur in the experiments.

Composite Subfloor Studies

Two static and two dynamic tests were conducted on the three composite subfloor specimens. With the skeleton subfloor, both static and dynamic tests to destruction were conducted. With the skinned subfloor, a nondestructive static test, followed by a dynamic test to failure, was conducted.

Static tests. Experimental results (ref. 34) for the skeleton subfloor specimen following a static test are shown in figure 20. As shown in figure 20(a), failures on the 3 Z-section frames occurred at 15 discrete locations. Unlike the unnotched single Z-frame, the failures in this specimen occurred at notches (which served as stress risers) in the frame, through which the stringer passed. However, as shown in figure 20(b), the failures were still near the point of load application (approximately 12°–14°) and at other circumferential locations of approximately 55°. In the absence of skin material, twisting and out-of-plane bending occurred with the frames. The stringers had minimal effect on the subfloor response, with the exception of maintaining the lateral spacing of the three Z-frames.

Dynamic tests. A photograph of a skeleton subfloor after impact onto a concrete surface at 20 ft/sec is shown in figure 21. In the dynamic test of the skeleton subfloor, fractures were produced at notches in the frames (fig. 21(a)) and, as shown in figure 21(b), also near the point of impact (about 14° because of the splice plate) and at 2 other locations up the circumference of the frames (45° and 78°), totaling 15 fractures for all 3 frames. The impact energy exceeded the energy absorbed by the local fractures, and the floor bottomed out in the impact. Figure 21(c) shows normalized circumferential strain distribution measured on the flange of the first (end) frame during the dynamic test just before first failure. A comparison of the distribution to the moment distribution of figures 17(b) and (c) shows essentially identical shape between the single frame and skeleton frame distributions. Maximum values at 0° and at approximately 50° to 55° agree well with the analytically predicted locations on the frame.

Impact results for the subfloor with skin after an impact of 20 ft/sec are shown in figure 22. A photograph of the subfloor specimen after the test is shown in figure 22(a). Points of failure of the frames in this specimen are indicated in figure 22(b). Again the points of failure are near the impact point (within 12°) and circumferentially at about 56° up both sides of the middle and rear frames and at 45°, 11.3°, and 22.5° on the front frame. It was observed that the subfloor impacted first on the front area, possibly explaining the 11.3° and 22.5° fractures being different from those at the other locations. Again all three frames were involved in the failures. Some delamination of the frames from the skin was evident, but the skin remained intact. A normalized circumferential strain distribution (just prior to first failure) measured on the skin at the first (end) frame during the dynamic test is shown in

figure 22(c). A comparison of the distribution with the moment distributions of figures 17(b) and (c) and the strain distribution in figure 21(c) shows essentially identical shape as the single frame and skeleton frame distributions. As was the case for the skeleton subfloor, maximum values at 0° and at approximately 50° to 55° agree well with the analytically predicted locations on the frame.

As mentioned previously in the frame studies, once the frames fail at or near the point of impact, the broken ends of the frame often jammed together and moved upward in a guided manner. In the subfloor structure, the frames may still fail completely across the section, but the skin remains intact and serves as a much less stiff boundary condition for the broken frames as the deflection increases. Little energy is involved in snapping the skin through as the load increases on the structure. (See ref. 35 on snap-through of composite arches.) In this manner, the structural stiffness of the frame and skin before fracture changes to only the skin after frame fracture. The analytical models discussed in the section "Static Analytical Studies" (p. 4) simulated this type of behavior.

Analytical studies. The contribution of the skin to the stiffness of the section with the nonsymmetrical frames is illustrated in figure 23. Static load deflection data for the unskinned subfloor and the skinned subfloor along with the DYCAST predictions are shown in the figure. It can be noted that the stiffness of the skinned subfloor is approximately three times the stiffness of the skeleton subfloor, thus the contribution of the skin to the structure is to maintain in-plane deflections of the nonsymmetrical Z-section and prevent any substantial twisting of the frames. Out-of-plane bending and twist were allowed in the skeleton subfloor predictions. As might be expected, if the skeleton subfloor load (with three frames) is reduced by a factor of three, good correlation with single frame load deflection data is evident.

General Observations

The response behavior determined during the studies of full-scale aircraft sections, fuselage panels, frames, and subfloors are summarized in figure 24. The normalized moment distribution on a representative frame of the various specimens is shown in figure 24(a) along with the failure locations (fig. 24(b)) from static and/or dynamic tests. The visual impression is quite striking among the various specimens. It is suggested from the results that for the simpler frames to the more complex subfloors and full-scale sections, a strong similarity is evident in the failure behavior of the structures. The structures share in common the generally circular or cylindrical shape, the vertical loading situations, and what appears to be a similar pattern of failure behavior. Analytical models of frame structures under vertical loads have moment distributions with maximums at the point of loading and at approximately 45° to 50° (depending on boundary conditions) around the circumference from the ground contact point. Failures of the structures were noted at these same locations. Such observations can help dynamists gain a clearer understanding of what to expect from such structures in crash loading situations, and they can help designers of new structures account for the vertical crash loads and allow increased energy absorption to be included in the new designs. Additionally, the observations can help analysts improve modeling of aircraft structures for predicting the failure responses and behavior under crash situations. The latter task is a difficult and challenging one, not only for composite structures but for metal structures as well. Studies are currently underway to improve the analysis capabilities of code and to add composite elements to finite element libraries such as the DYCAST program. In addition, new analysis approaches are being explored through grants to universities as an extension of Langley Research Center's efforts.

Concluding Remarks and Observations

Some important failure behavior results from research with composite full-scale aircraft sections, composite structural elements, and subfloors have been presented. Observations on the failure behavior of these structures have been made and discussed, and analytical results have been included to help explain some of the behavior noted.

From the observations made in the overview, the following conclusions are made:

1. Comparing test results on simple representative structural elements with those from more complex components provided insight into the local and global structural responses and behavior of complex aircraft structures.
2. Relatively simple analytical models provided generally good correlation with experiments. However, guidance from experimental data was required to allow adequate or improved analytical models to be formulated.
3. Commonality in the failure behavior of full-scale aircraft sections, composite panels, frames, and subfloors with and without skin was found.
4. General locations of failures appear to occur at the same structural regions among the specimens as a result of similar geometry (cylindrical shape),

loading (vertical), and moment (stress/strain) distribution on the structures under vertical loads.

5. Noted failures were located in the same regions as the maximums in the moment (strain) distribution on the structures.
6. The shape of the distribution of the moment was independent of the size (diameter) of the frame or component. The loads, however, that produced the failures varied with the structural size.
7. Loading the frames having floors attached at different circumferential locations produced similar moment distributions, but the maximum moment locations away from the contact region (as expected) were lower in circumferential position than the full half-circle frame results. Maximum moments for the lower floor attachment locations were lower in magnitude (for a given load) than for the full 180° frame.

Based on the conclusions drawn for the research presented in this paper, the following observations are also summarized:

1. The general similarity of the failure behavior can (a) assist designers and dynamists to anticipate how the structures probably will fail, (b) provide guidance on how and where to incorporate and/or optimize improved energy absorption into new structural designs, and (c) aid analysts to more adequately model the structures for predicting failure and load behavior under crash situations.
2. To analytically predict, in a dynamic loading situation, the complex failure events and the loads that initiate failures in composite structural elements and subcomponents is a challenge, but possible; however, guidance is often required from experiments.
3. Composite curved beam, composite plate, and shell elements are being developed and included in finite element code to improve the capability to analyze composite structures.

NASA Langley Research Center
Hampton, VA 23665-5225
August 22, 1990

References

1. Alfaro-Bou, Emilio; and Vaughan, Victor L., Jr.: *Light Airplane Crash Tests at Impact Velocities of 13 and 27 m/sec.* NASA TP-1042, 1977.
2. Castle, Claude B.; and Alfaro-Bou, Emilio: *Light Airplane Crash Tests at Three Flight-Path Angles.* NASA TP-1210, 1978.
3. Hayduk, Robert J.: *Comparative Analysis of PA-31-350 Chieftain (N44LV) Accident and NASA Crash Test Data.* NASA TM-80102, 1979.
4. Castle, Claude B.; and Alfaro-Bou, Emilio: *Light Airplane Crash Tests at Three Roll Angles.* NASA TP-1477, 1979.
5. Vaughan, Victor L., Jr.; and Alfaro-Bou, Emilio: *Light Airplane Crash Tests at Three Pitch Angles.* NASA TP-1481, 1979.
6. Vaughan, Victor L., Jr.; and Hayduk, Robert J.: *Crash Tests of Four Identical High-Wing Single-Engine Airplanes.* NASA TP-1699, 1980.
7. Carden, Huey D.; and Hayduk, Robert J.: *Aircraft Subfloor Response to Crash Loadings.* SAE Tech. Paper Ser. 810614, Apr. 1981.
8. Williams, M. Susan; and Fasanella, Edwin L.: *Crash Tests of Four Low-Wing Twin-Engine Airplanes With Truss-Reinforced Fuselage Structure.* NASA TP-2070, 1982.
9. Carden, Huey D.: *Correlation and Assessment of Structural Airplane Crash Data With Flight Parameters at Impact.* NASA TP-2083, 1982.
10. Carden, Huey D.: *Impulse Analysis of Airplane Crash Data With Consideration Given to Human Tolerance.* SAE Tech. Paper Ser. 830748, Apr. 1983.
11. Castle, Claude B.; and Alfaro-Bou, Emilio: *Crash Tests of Three Identical Low-Wing Single-Engine Airplanes.* NASA TP-2190, 1983.
12. Thomson, Robert G.; Carden, Huey D.; and Hayduk, Robert J.: *Survey of NASA Research on Crash Dynamics.* NASA TP-2298, 1984.
13. Carden, Huey D.: *Full-Scale Crash-Test Evaluation of Two Load-Limiting Subfloors for General Aviation Airframes.* NASA TP-2380, 1984.
14. Hayduk, Robert J., compiler: *Full-Scale Transport Controlled Impact Demonstration.* NASA CP-2395, 1986.
15. Fasanella, Edwin L.; Widmayer, E.; and Robinson, Martha P.: Structural Analysis of the Controlled Impact Demonstration of a Jet Transport Airplane. AIAA-86-0939, May 1986.
16. Fasanella, Edwin L.; Alfaro-Bou, Emilio; and Hayduk, Robert J.: *Impact Data From a Transport Aircraft During a Controlled Impact Demonstration.* NASA TP-2589, 1986.
17. Farley, Gary L.: *Energy Absorption of Composite Materials.* NASA TM-84638, AVRADCOM TR-83-B-2, 1983.
18. Bannerman, D. C.; and Kindervater, C. M.: *Crashworthiness Investigation of Composite Aircraft Subfloor Beam Sections.* IB 435-84/3 (1984), Deutsche Forschungs - und Versuchsanstalt für Luft- und Raumfahrt, February 1984.
19. Cronkhite, J. D.; Chung, Y. T.; and Bark, L. W.: *Crashworthy Composite Structures.* USAAVSCOM TR-87-D-10, U.S. Army, Dec. 1987. (Available from DTIC as AD B121 522.)
20. Jones, Lisa E.; and Carden, Huey D.: *Evaluation of Energy Absorption of New Concepts of Aircraft Composite Subfloor Intersections.* NASA TP-2951, 1989.
21. Vaughan, Victor L., Jr.; and Alfaro-Bou, Emilio: *Impact Dynamics Research Facility for Full-Scale Aircraft Crash Testing.* NASA TN D-8179, 1976.
22. Pifko, A. B.; Winter, R.; and Ogilvie, P. L.: *DYCAST—A Finite Element Program for the Crash Analysis of Structures.* NASA CR-4040, 1987.

23. Noor, Ahmed K.; and Peters, Jeanne M.: Model-Size Reduction for the Non-Linear Dynamic Analysis of Quasi-Symmetric Structures. *Eng. Comput.,* vol. 4, no. 3, Sept. 1987, pp. 178–189.
24. Noor, Ahmed K.; and Peters, Jeanne M.: A Computational Strategy for Making Complicated Structural Problems Simple. AIAA-88-2283, Apr. 1988.
25. Noor, Ahmed K.; Peters, Jeanne M.; and Min, Byung-Jin: *Mixed Finite Element Model for Free Vibrations of Thin-Walled Beams.* NASA TP-2868, 1989.
26. Williams, M. Susan; and Hayduk, Robert J.: *Vertical Drop Test of a Transport Fuselage Section Located Forward of the Wing.* NASA TM-85679, 1983.
27. Fasanella, Edwin L.; and Alfaro-Bou, Emilio: *Vertical Drop Test of a Transport Fuselage Section Located Aft of the Wing.* NASA TM-89025, [1986].
28. Cronkhite, James D.; and Mazza, L. T.: Bell ACAP Full-Scale Aircraft Crash Test and KRASH Correlation. Paper presented at 44th Annual Forum and Technology Display meeting of American Helicopter Soc. (Washington, D.C.), June, 1988.
29. Cronkhite, James D.; and Mazza, L. T.: KRASH Analysis Correlation with the Bell ACAP Full-Scale Aircraft Crash Test. Paper presented at Meeting on Advanced Rotorcraft Structures meeting of American Helicopter Soc. (Williamsburg, Virginia), Oct. 1988.
30. Jackson, A. C.; Balena, F. J.; LaBarge, W. L.; Pei, G.; Pitman, W. A.; and Wittlin, G.: *Transport Composite Fuselage Technology—Impact Dynamics and Acoustic Transmission.* NASA CR-4035, 1986.
31. Boitnott, Richard L.; and Kindervater, Cristof: Crashworthy Design of Helicopter Composite Airframe Structure. Fifteenth European Rotorcraft Forum, Paper no. 93, Sept. 1989.
32. Van den Broek, J. A.: *Elastic Energy Theory,* Second ed., John Wiley & Sons, Inc., c.1942.
33. Boitnott, Richard L.; Fasanella, Edwin L.; Calton, Lisa E.; and Carden, Huey D.: *Impact Response of Composite Fuselage Frames.* SAE Paper 871009, Apr. 1987.
34. Boitnott, Richard L.; and Fasanella, Edwin L.: *Impact Evaluation of Composite Floor Sections.* SAE Paper 891018, Apr. 1989.
35. Carper, Douglas M.; Hyer, Michael W.; and Johnson, Eric R.: *Large Deformation Behavior of Long Shallow Cylindrical Composite Panels.* VPI-E-83-37, Virginia Polytech. Inst. & State Univ., Sept. 1983.

ORIGINAL PAGE
BLACK AND WHITE PHOTOGRAPH

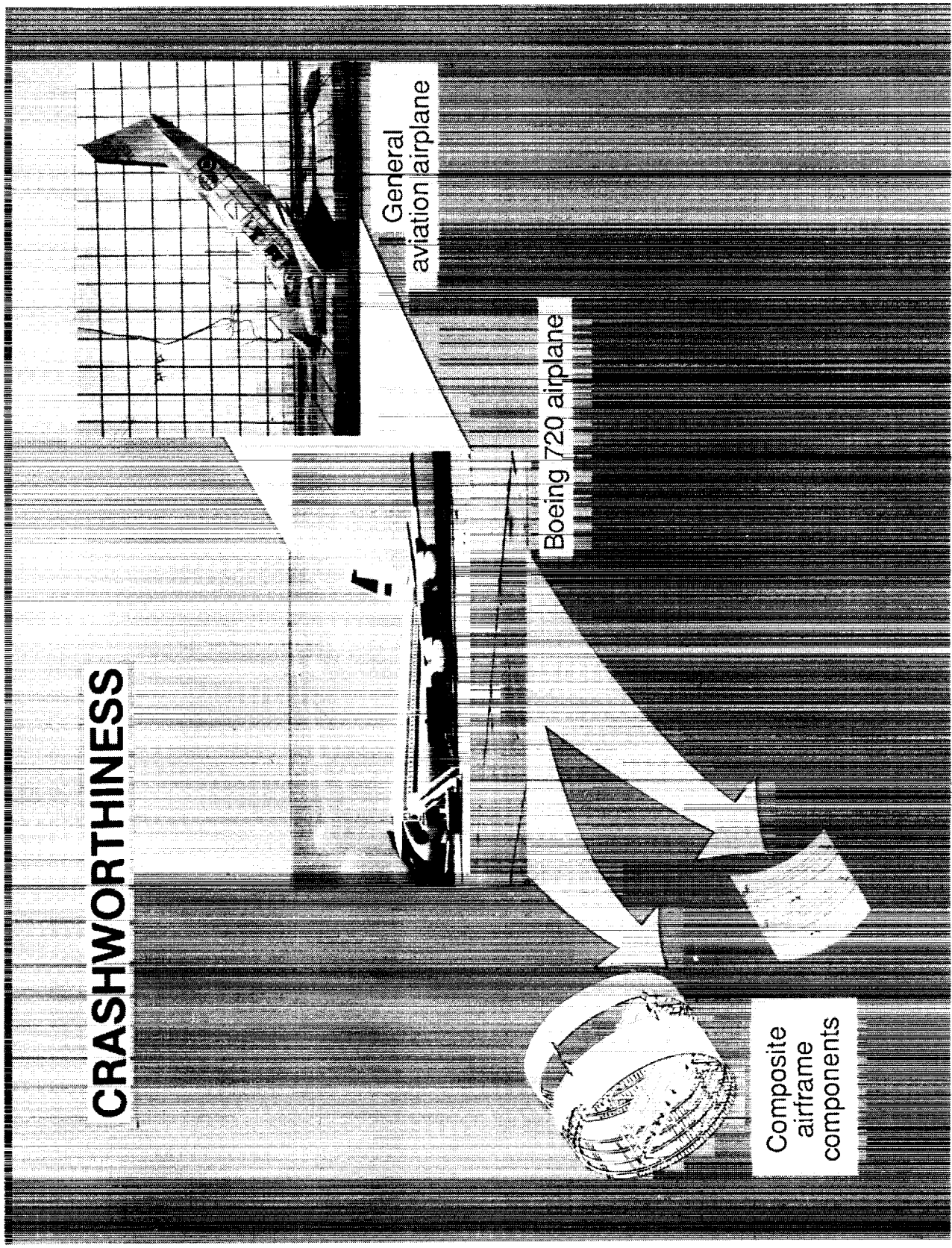

Figure 1. Progression of research areas in crash dynamics at Langley Research Center.

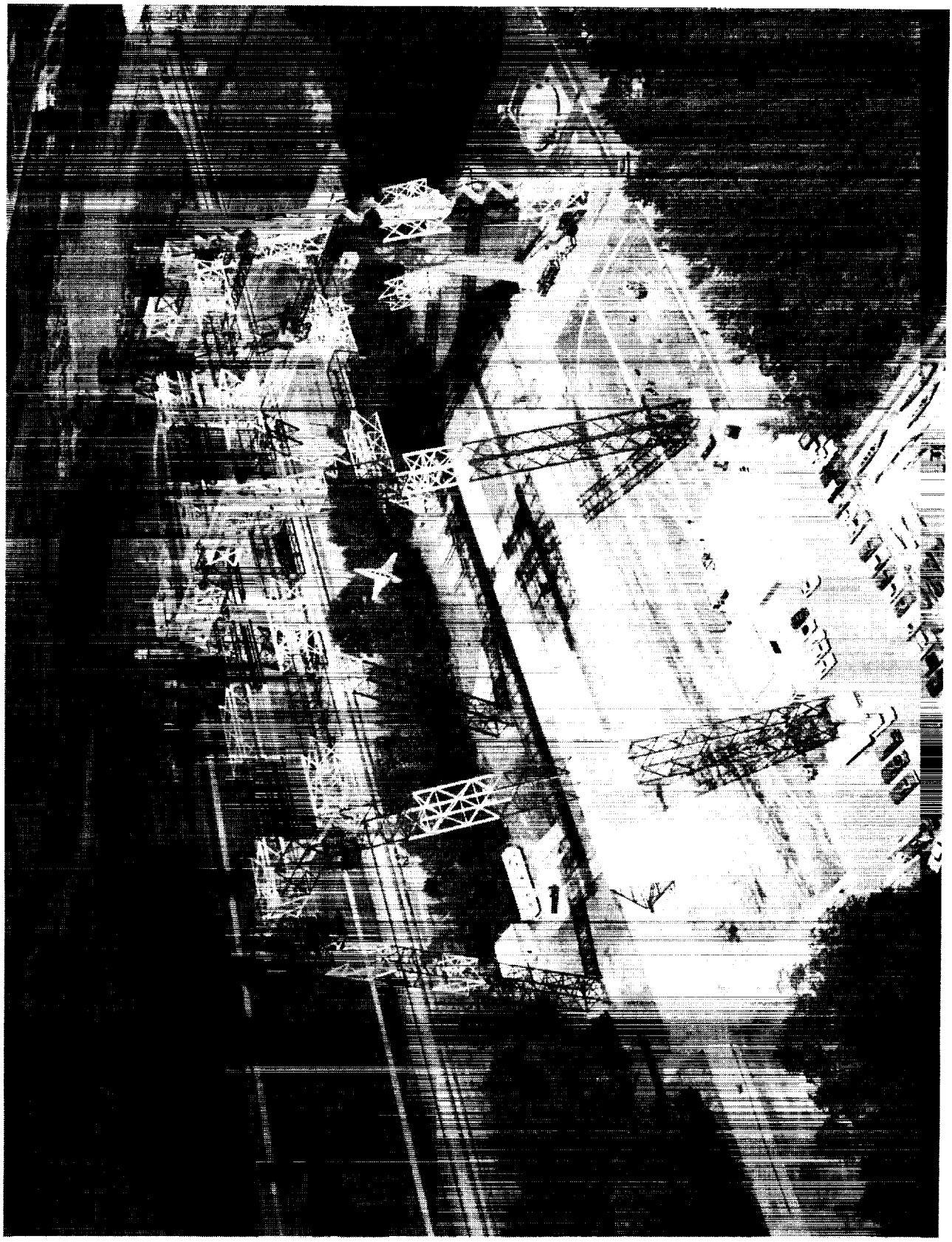

L-74-2505

Figure 2. Impact Dynamics Research Facility (IDRF) at Langley Research Center.

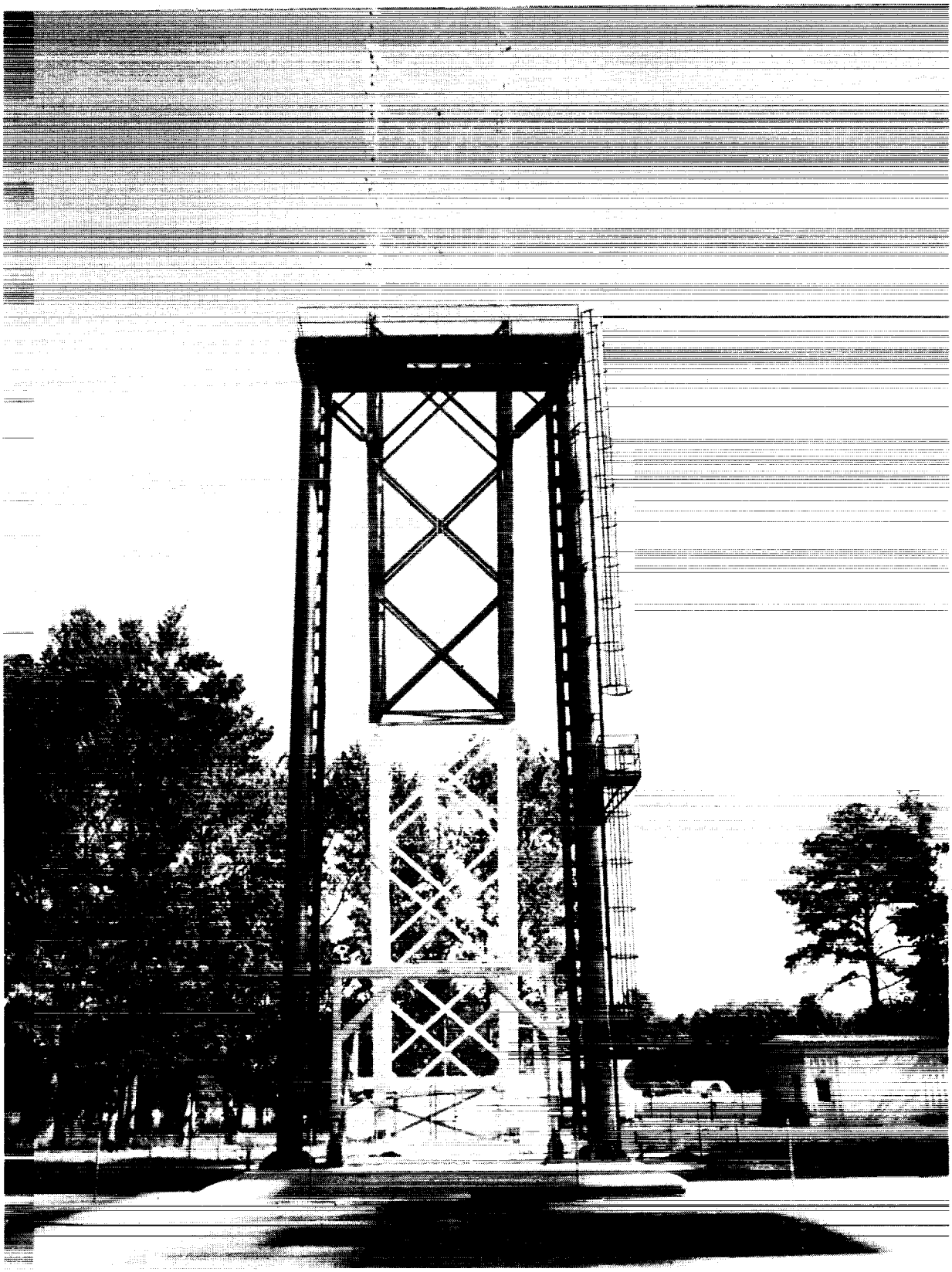

L-81-7816

Figure 3. Vertical Drop Test Apparatus used for component testing.

ORIGINAL PAGE
BLACK AND WHITE PHOTOGRAPH

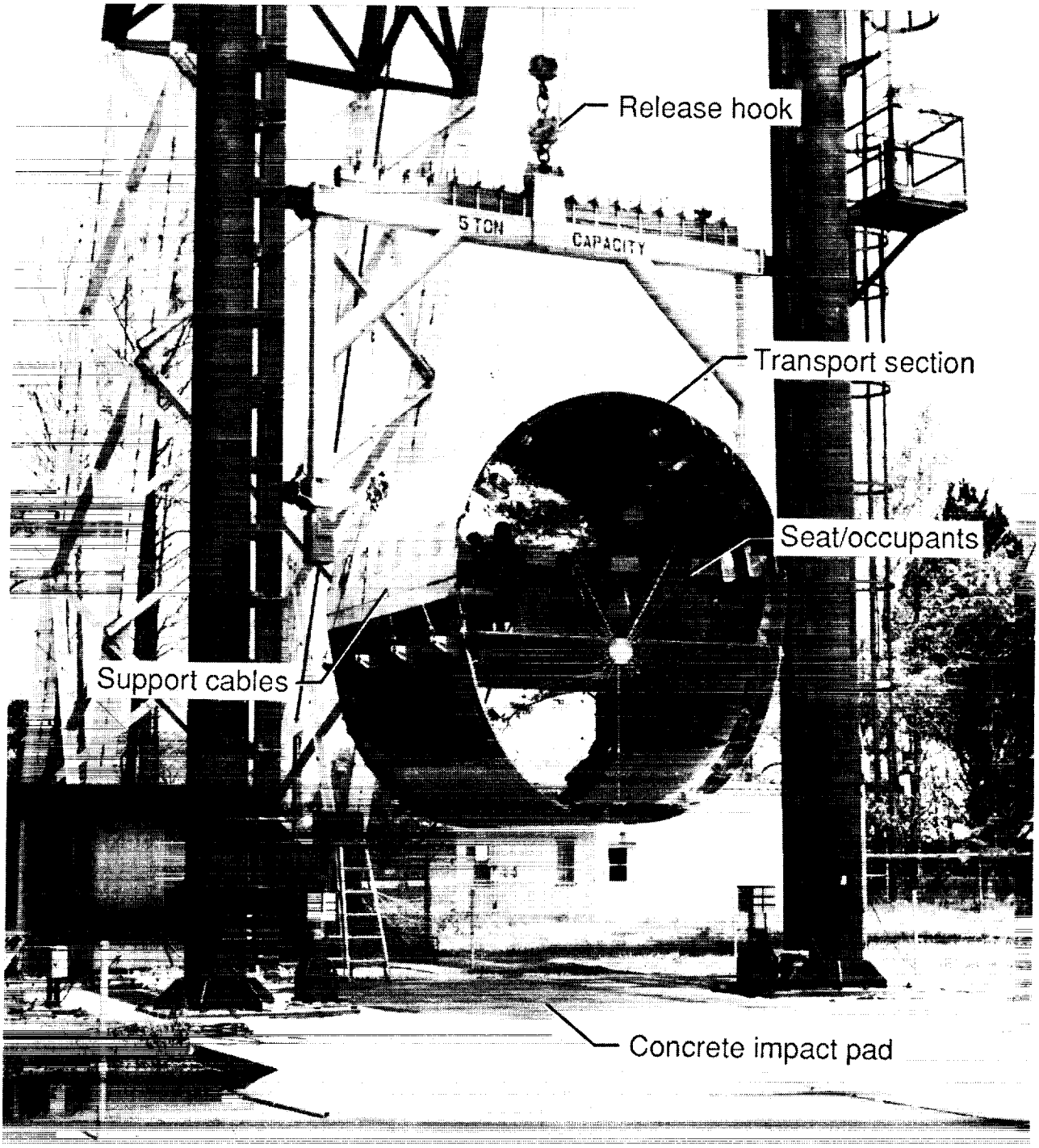

L-83-4199

Figure 4. Metal transport section suspended in Vertical Drop Test Apparatus.

ORIGINAL PAGE
BLACK AND WHITE PHOTOGRAPH

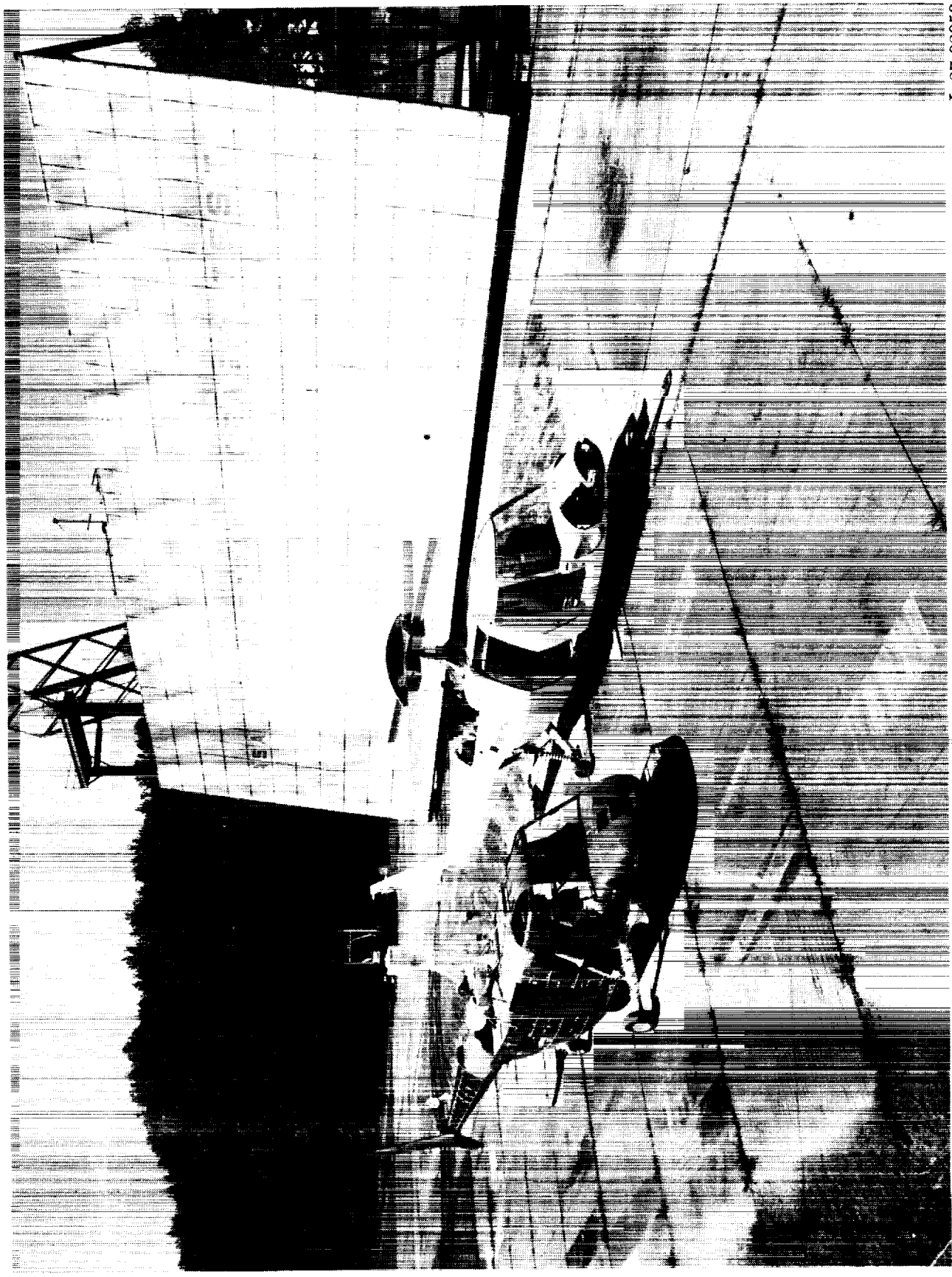

L-87-08053

Figure 5. Two Advanced Composite Aircraft Program (ACAP) structures.

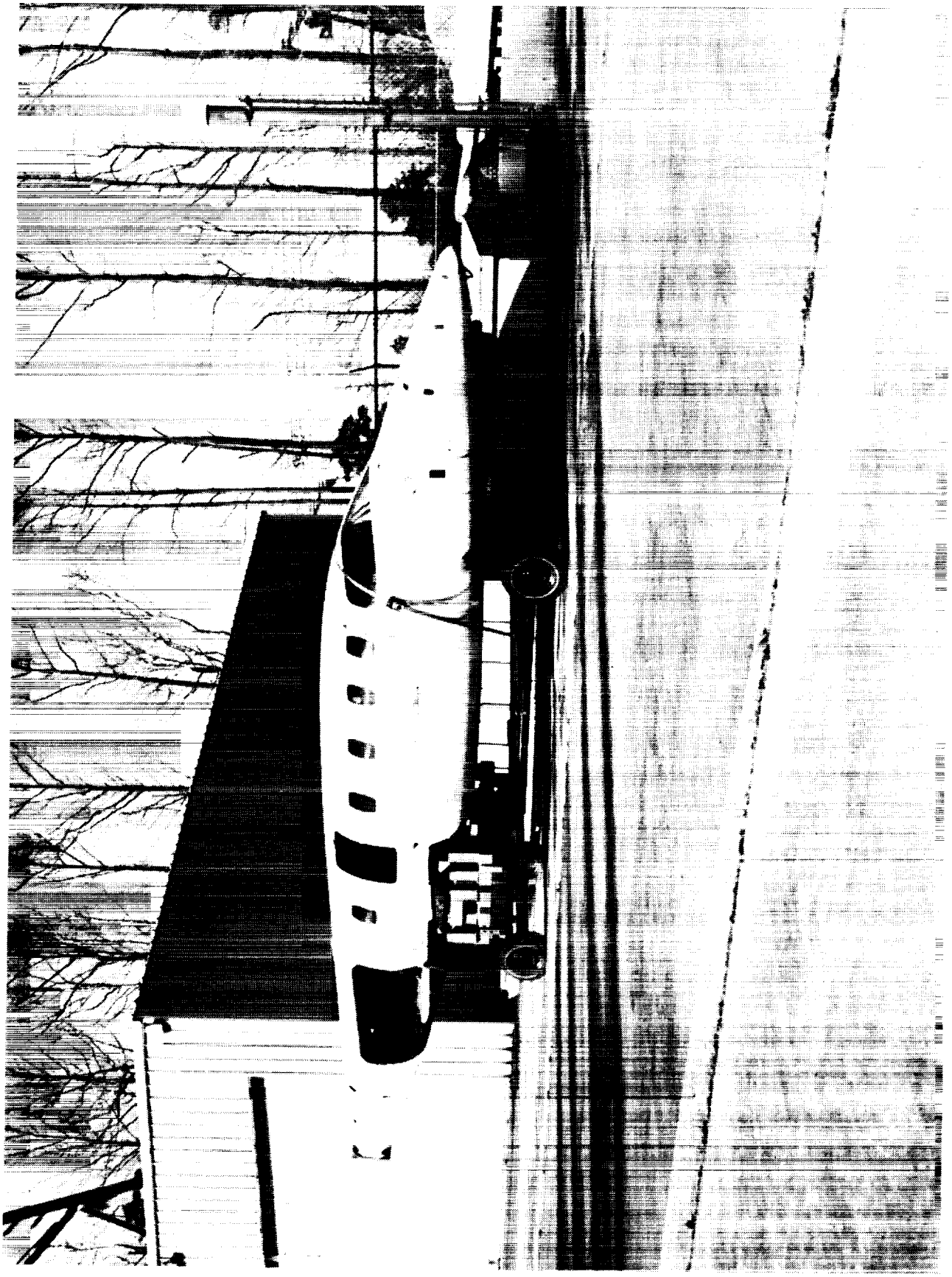

L-88-11364

Figure 6. Composite general aviation aircraft structure.

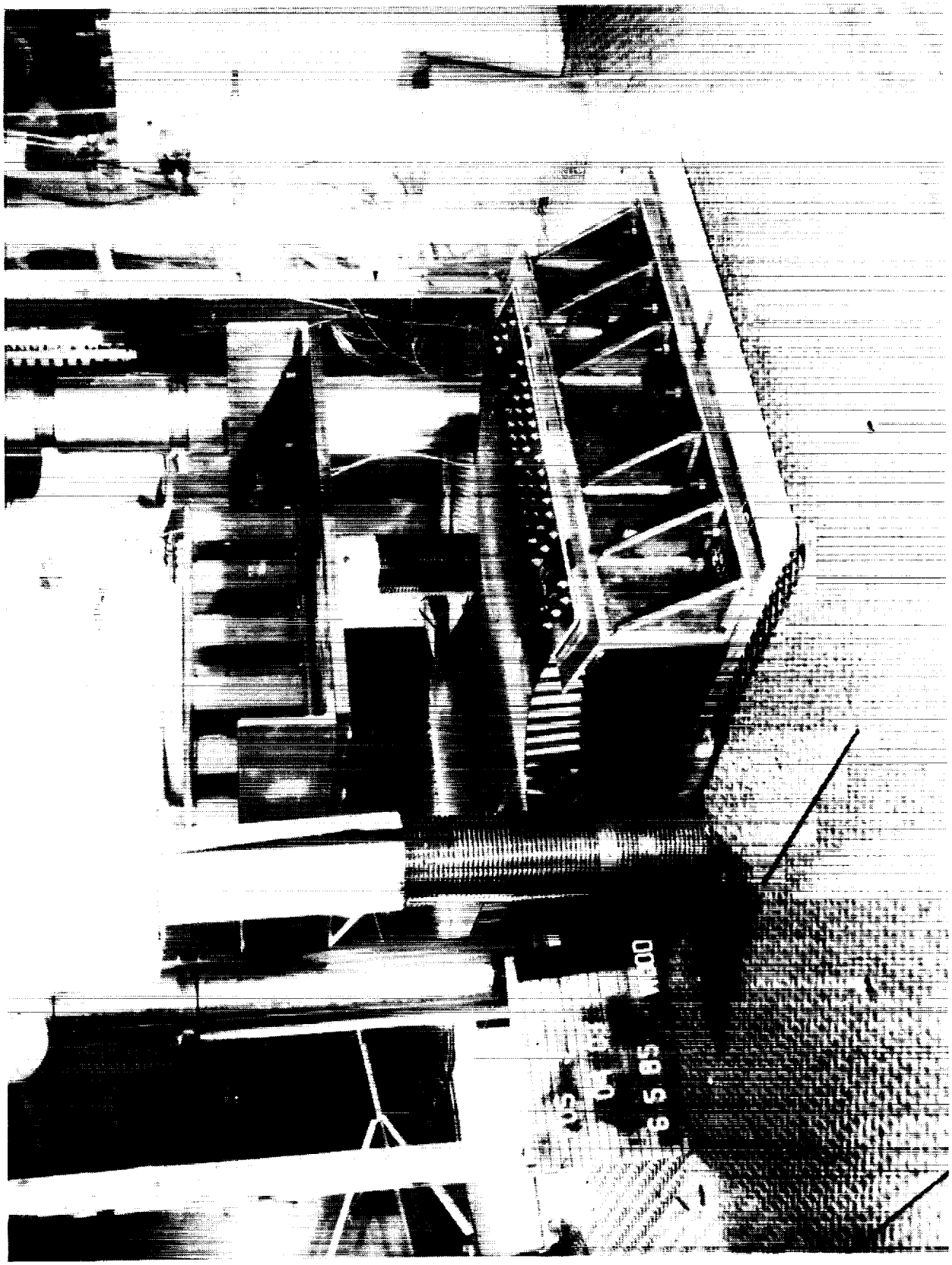

L-89-4474

Figure 7. Composite fuselage panel test specimen from Aircraft Energy Efficiency (ACEE) Program.

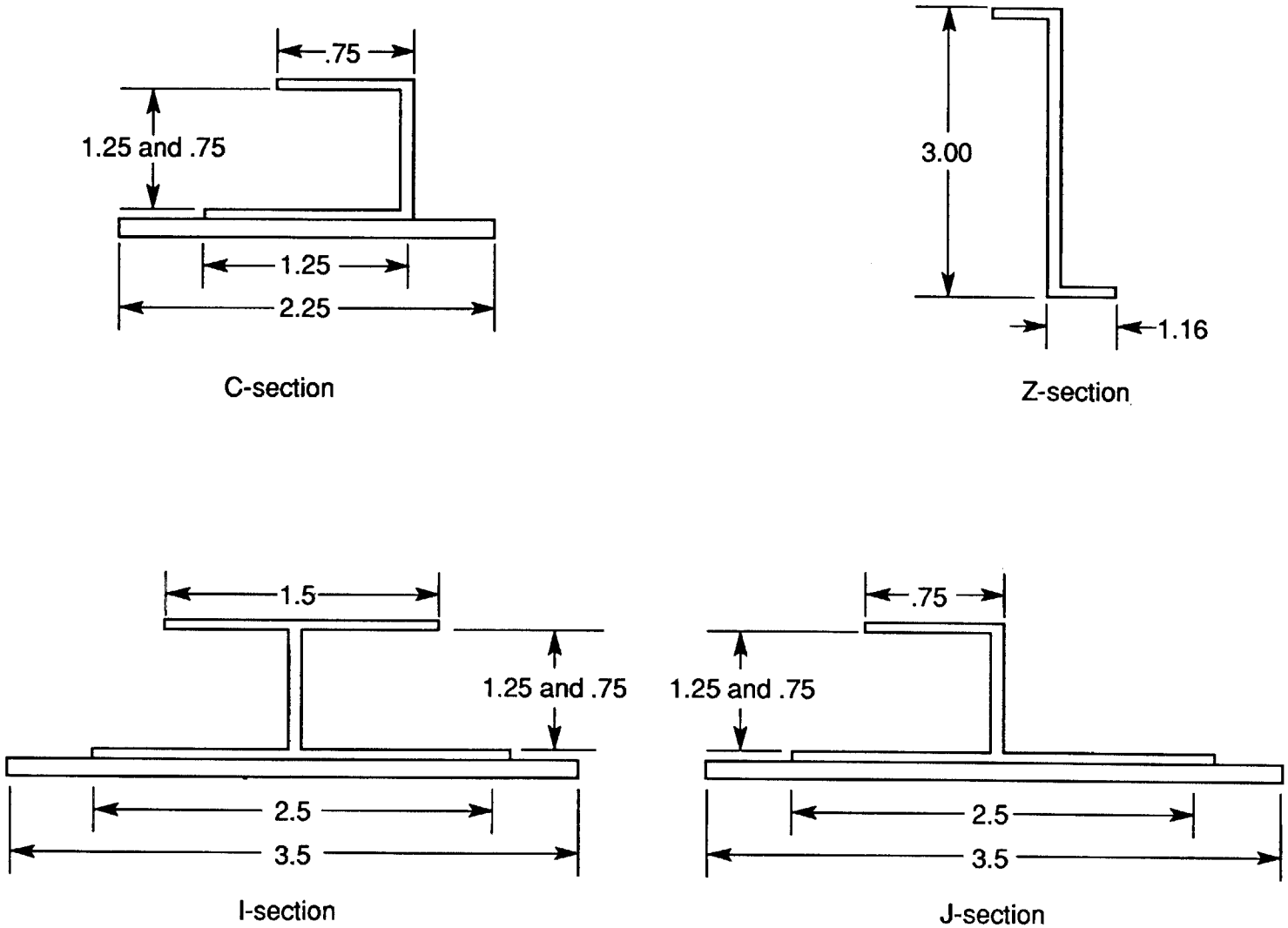

(a) Cross-sectional dimensions (in inches).

Figure 8. Various cross-sectional shapes of composite fuselage frames.

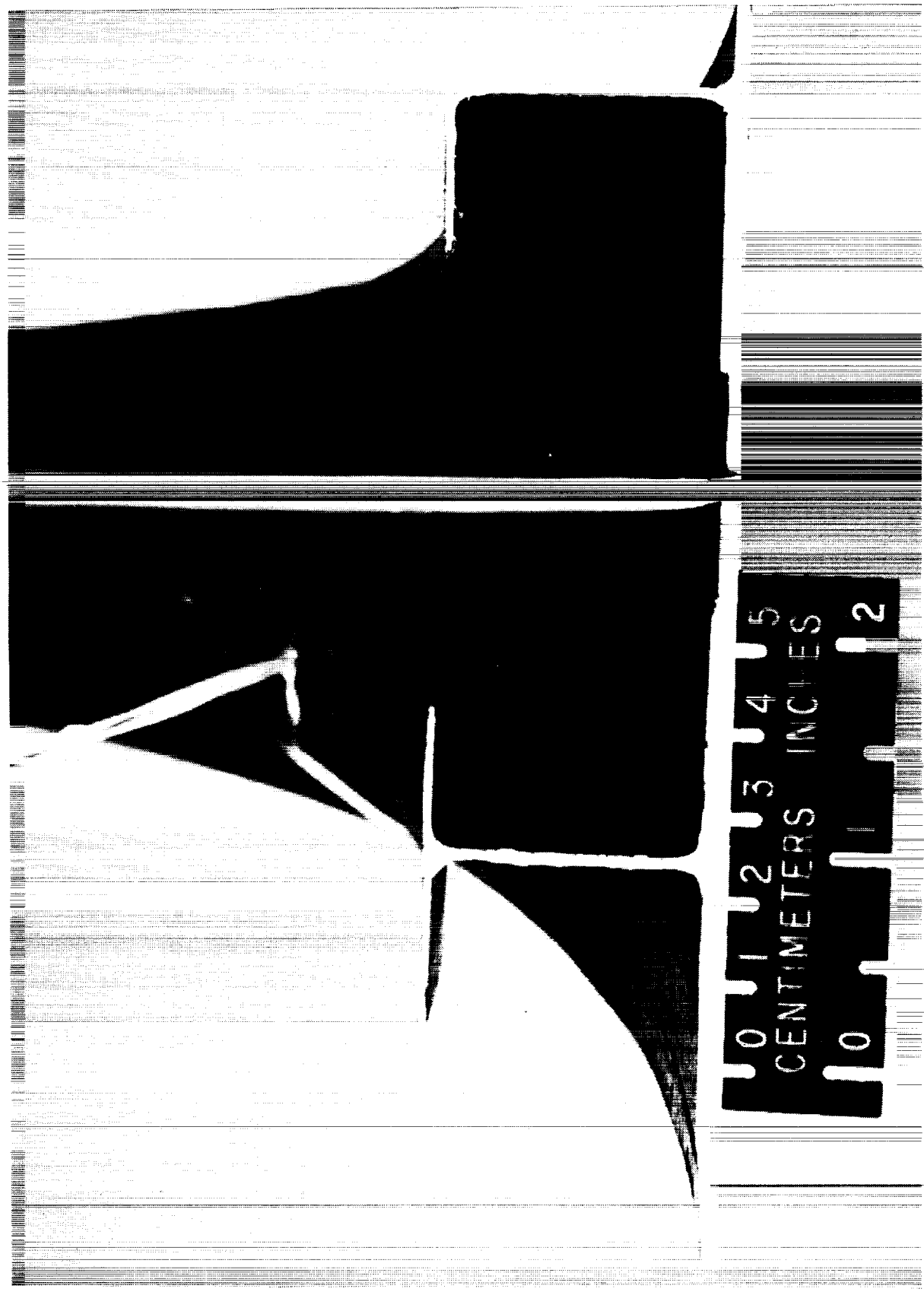

L-88-8658

(b) I- and C-cross section frames.

Figure 8. Continued.

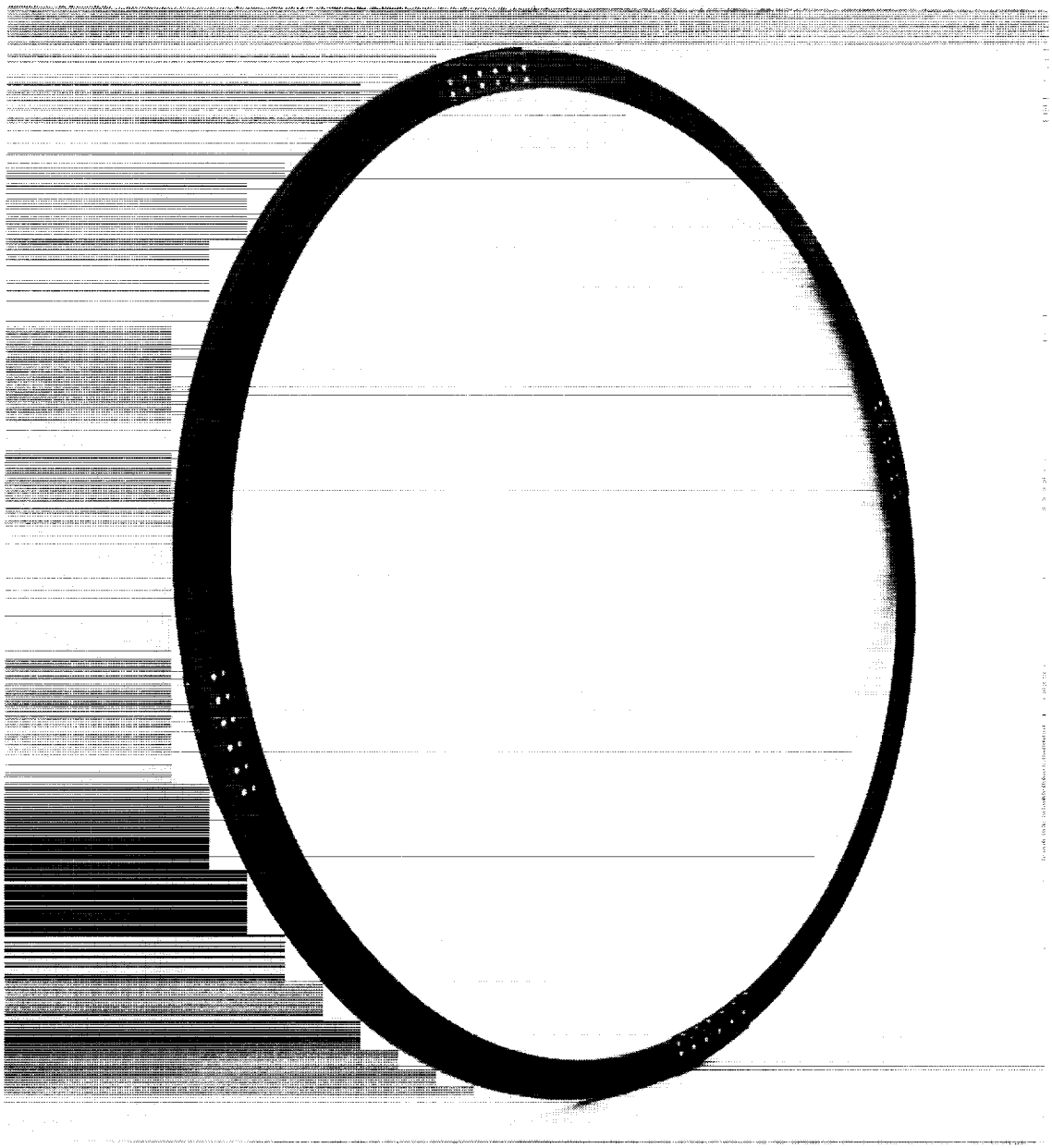

L-84-5662

(c) Z-cross section fuselage frame.

Figure 8. Concluded.

ORIGINAL PAGE
BLACK AND WHITE PHOTOGRAPH

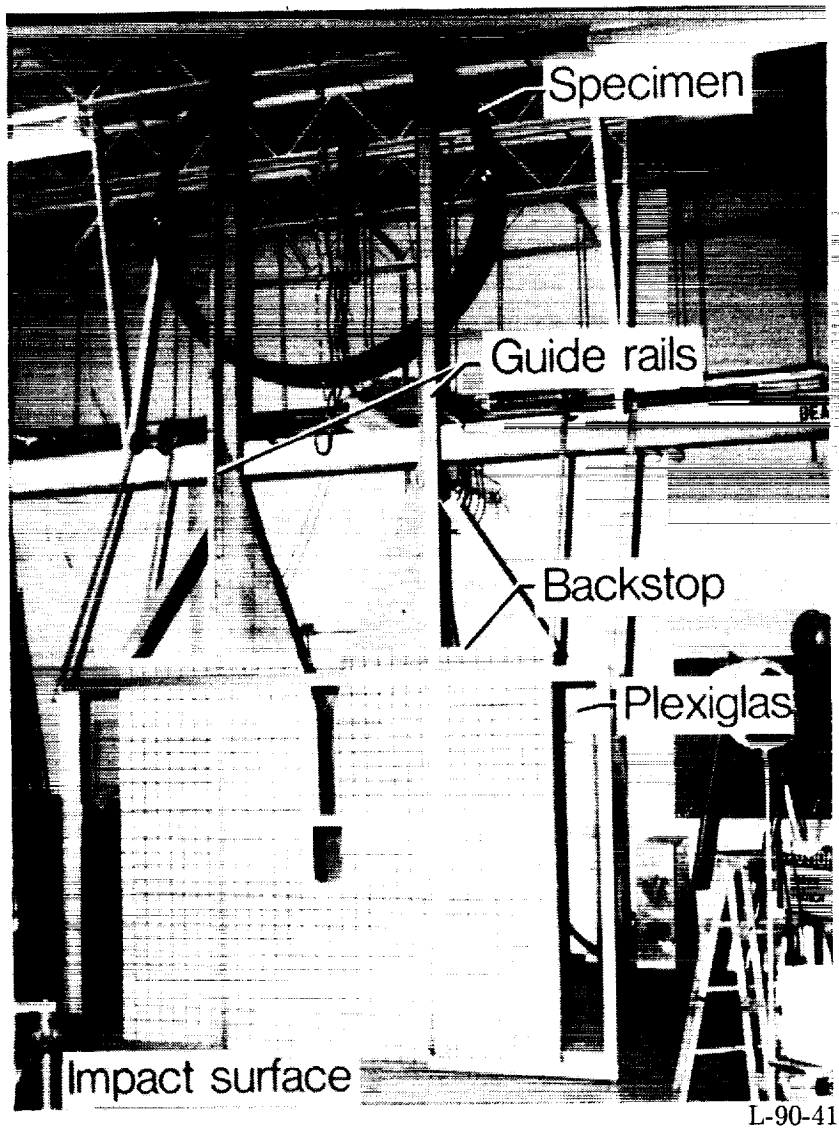

Figure 9. Composite Z-frame in drop test apparatus.

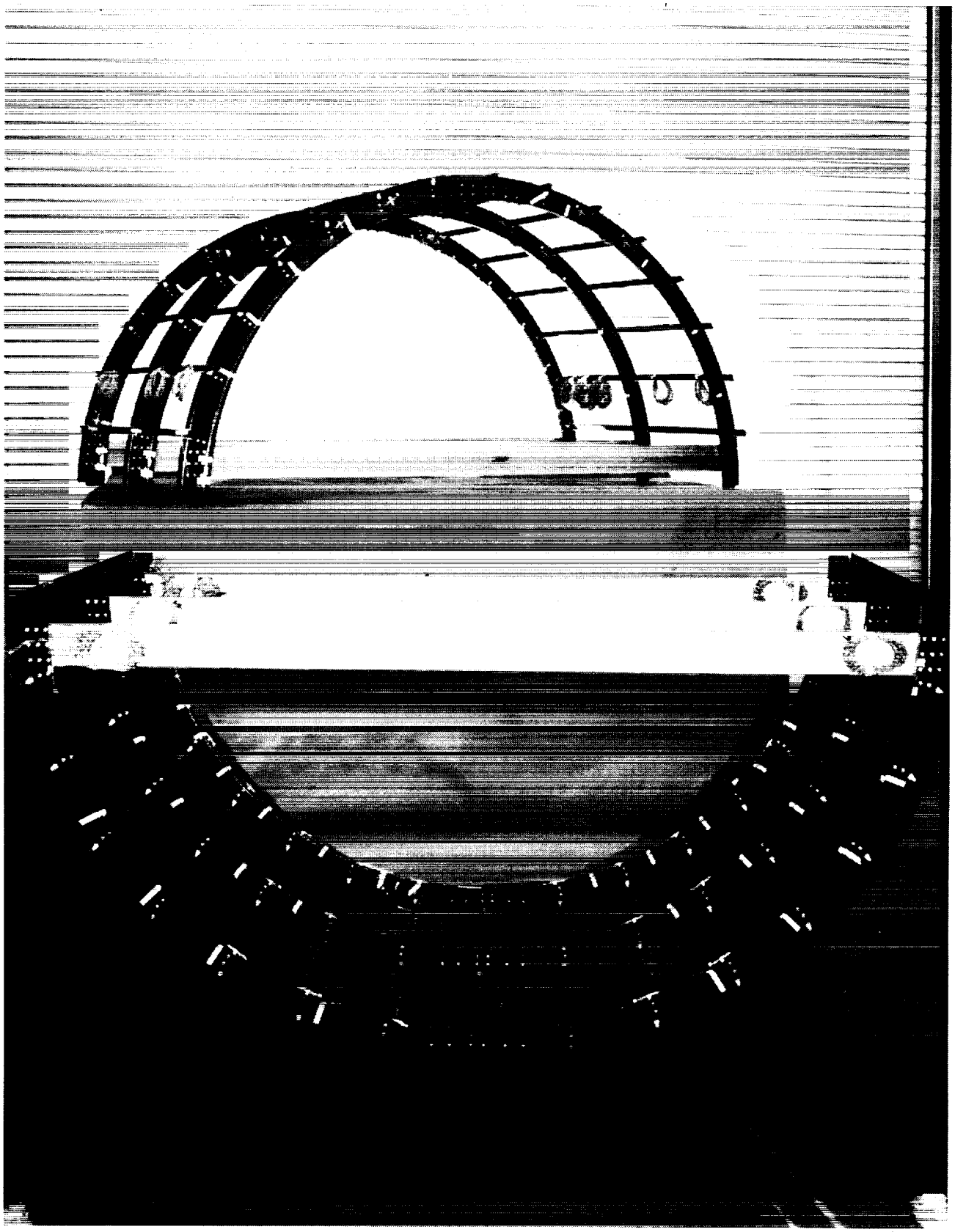

L-88-2037

Figure 10. Skeleton and skinned subfloor specimens.

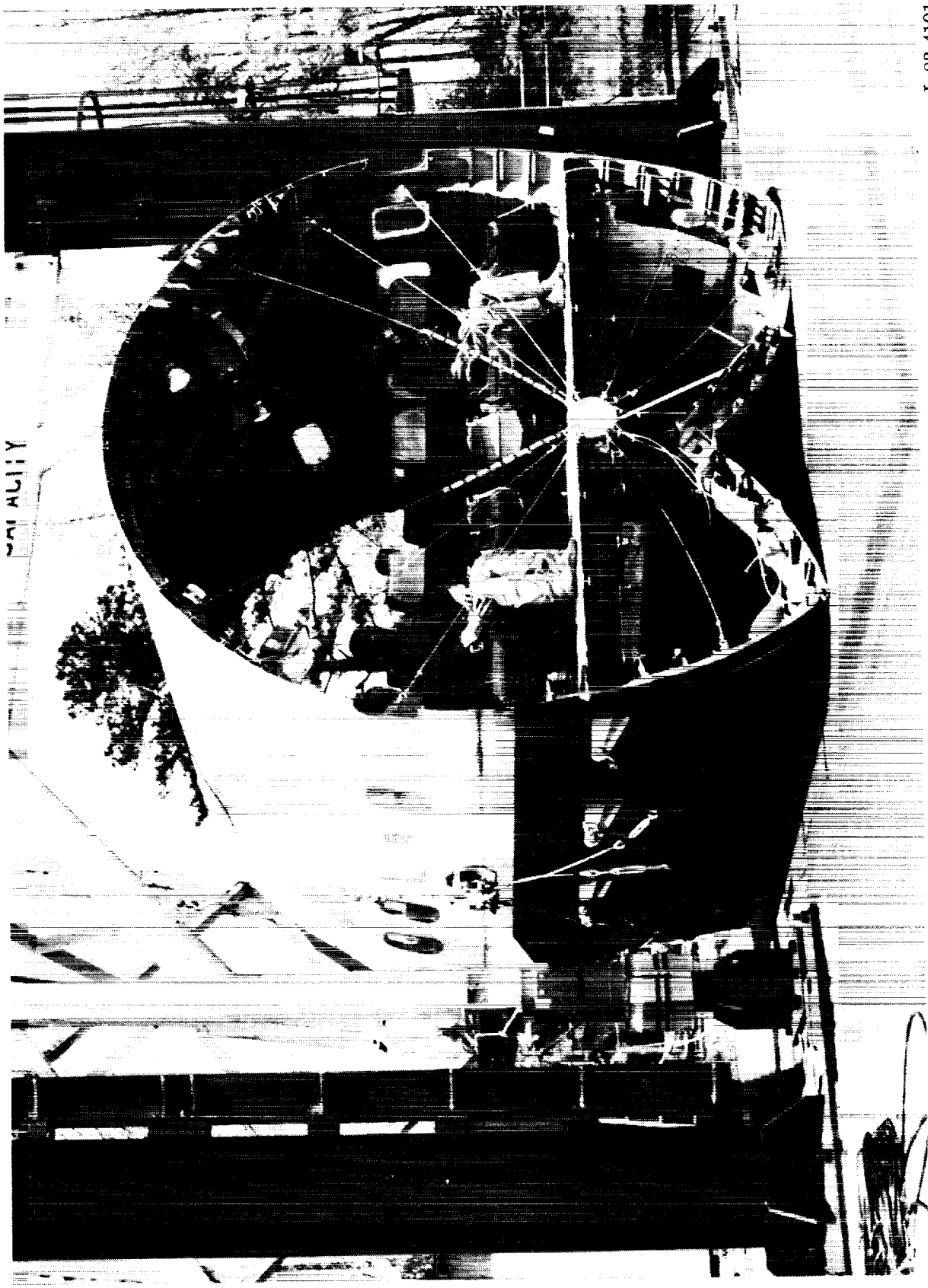

L-83-4191

(a) Section from forward of wing.

Figure 11. Structural damage to metal transport aircraft structures resulting from impact tests.

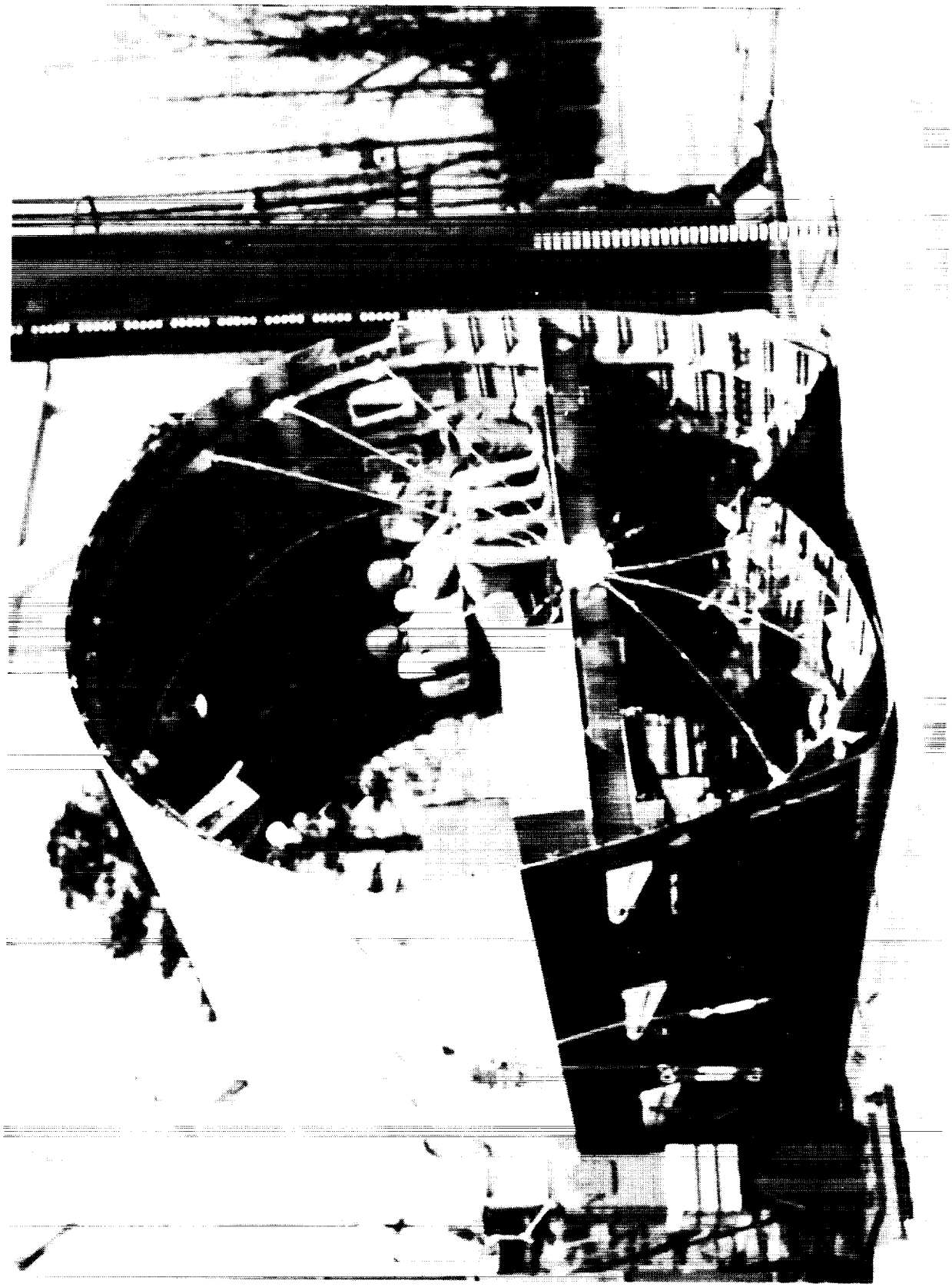

L-84-2899

(b) Section from aft of wing.

Figure 11. Continued.

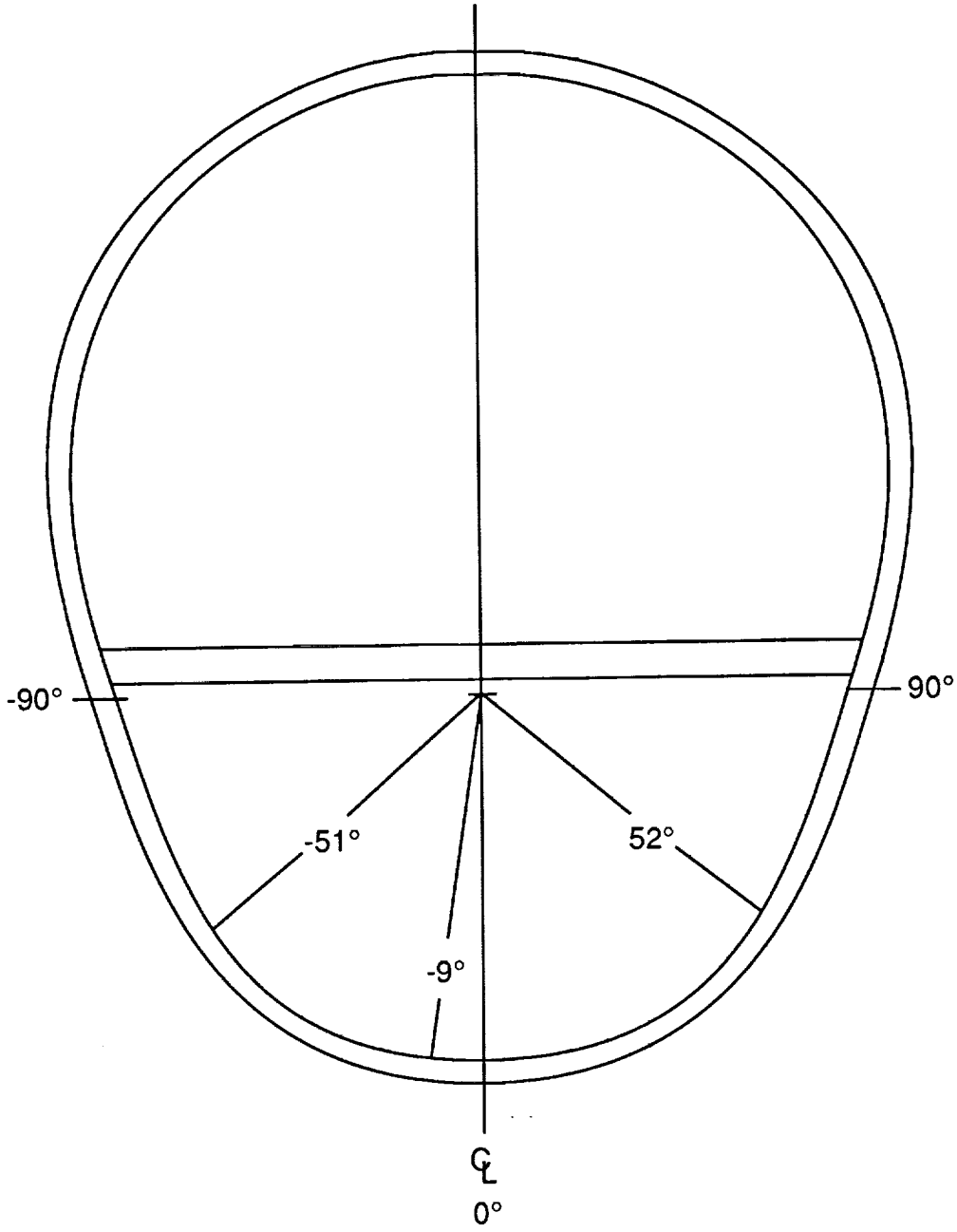

(c) Angular location of failures.

Figure 11. Concluded.

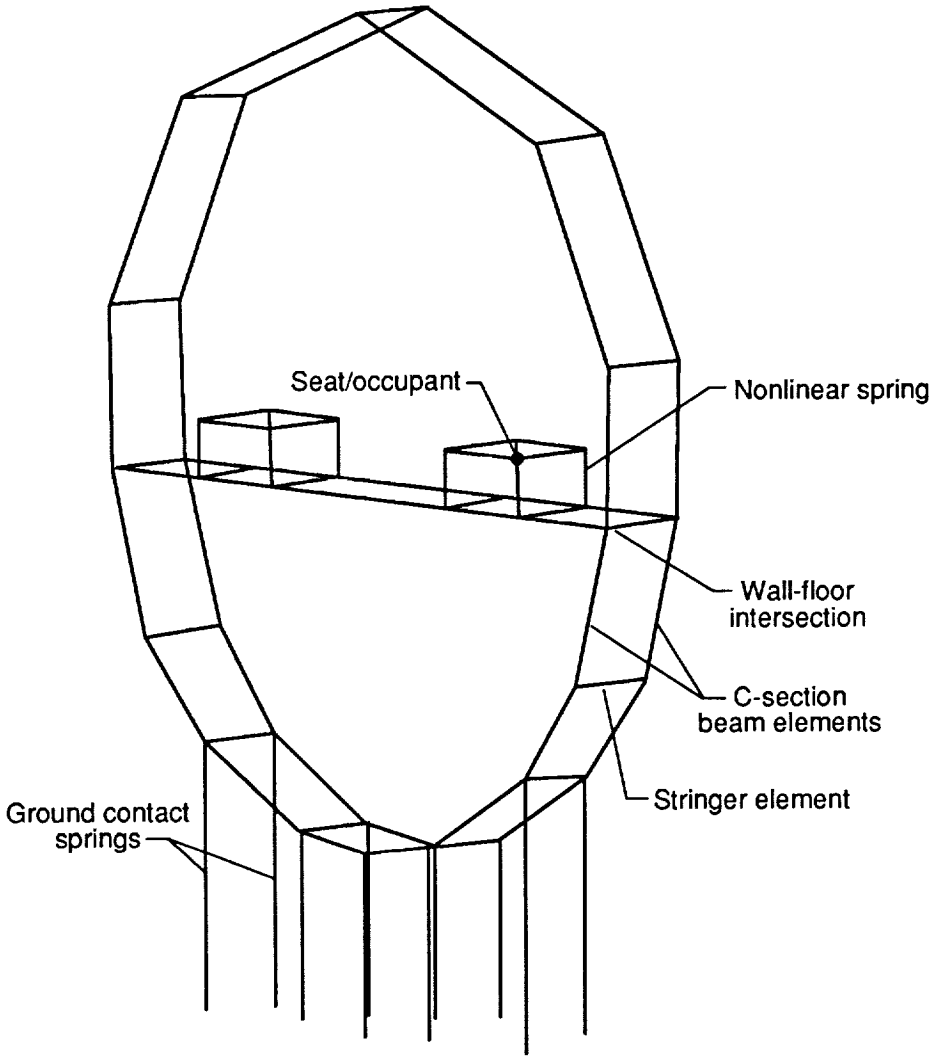

Figure 12. Finite element two-frame model of metal transport section.

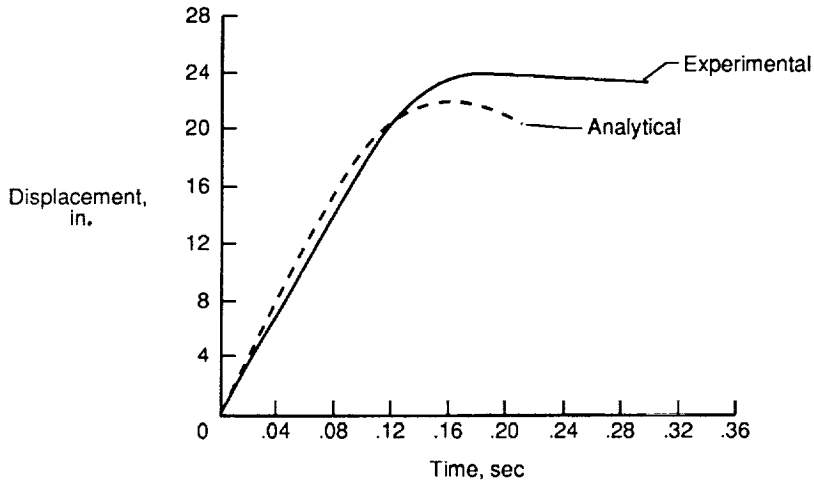

(a) Vertical floor displacements.

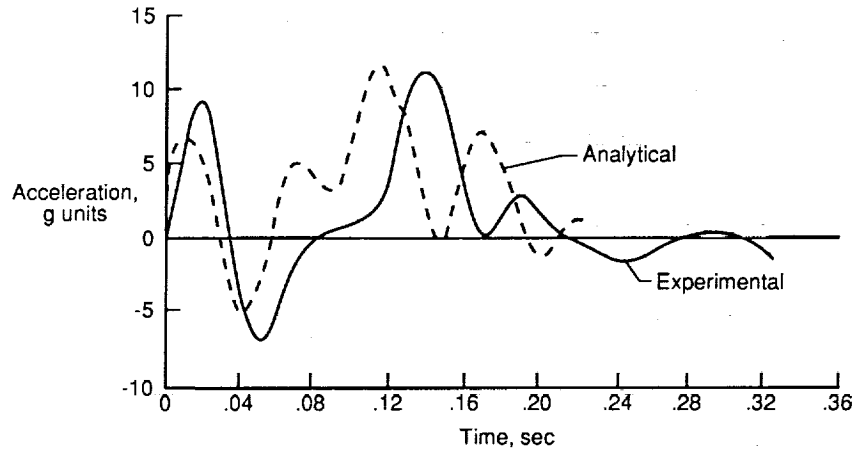

(b) Vertical accelerations at wall floor interface.

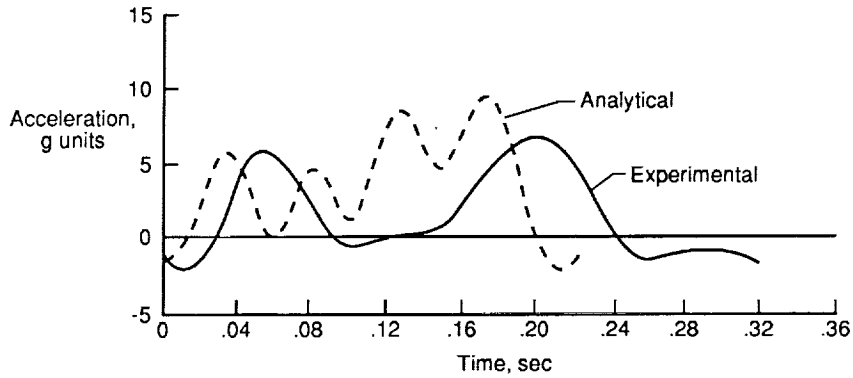

(c) Vertical pelvis accelerations.

Figure 13. Comparison of experimental and analytical fuselage crushing and accelerations of metal transport section.

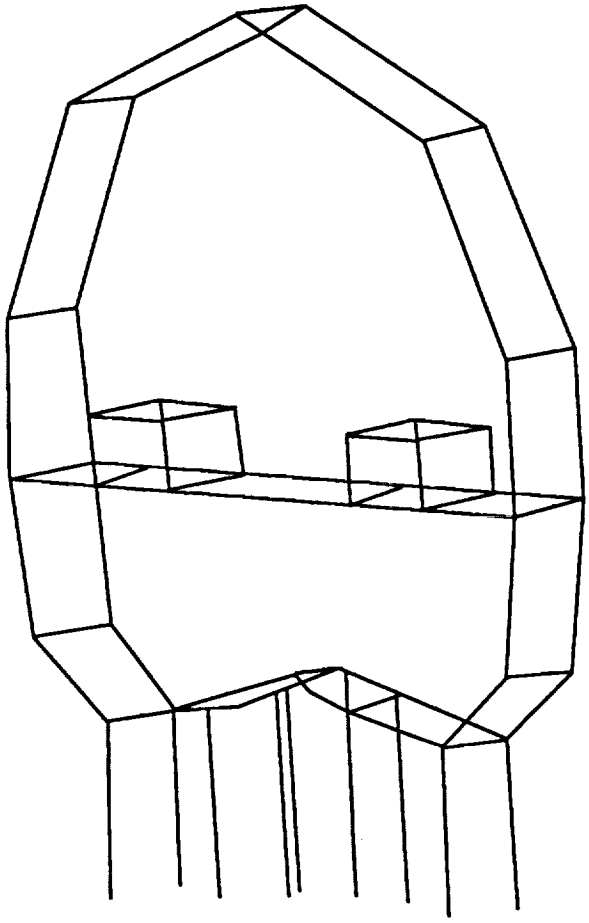

Figure 14. Deformed model showing analytical failure of metal transport section.

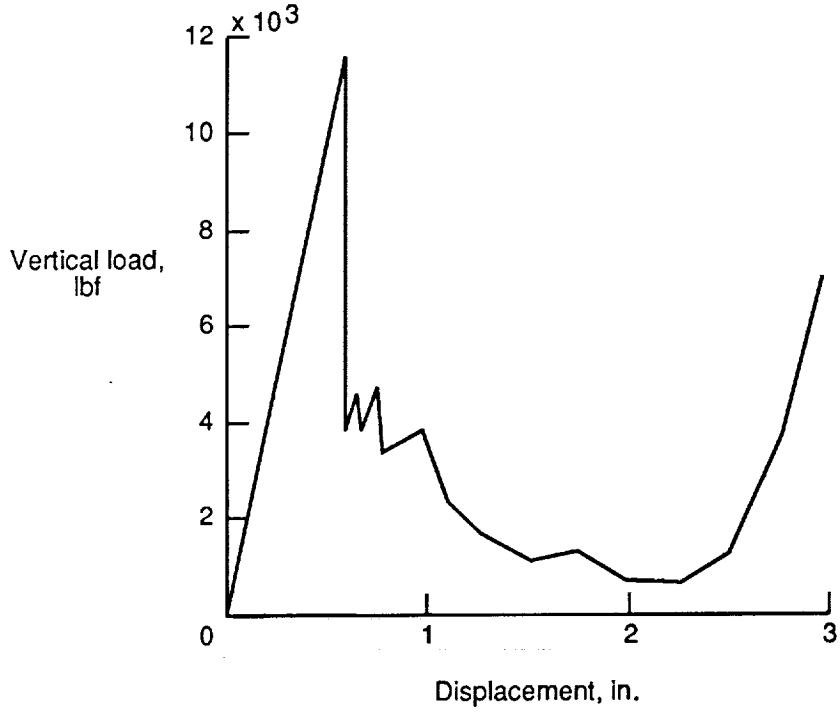

(a) Load deflection of composite panel.

Figure 15. Static results for composite frame/skin panel studies.

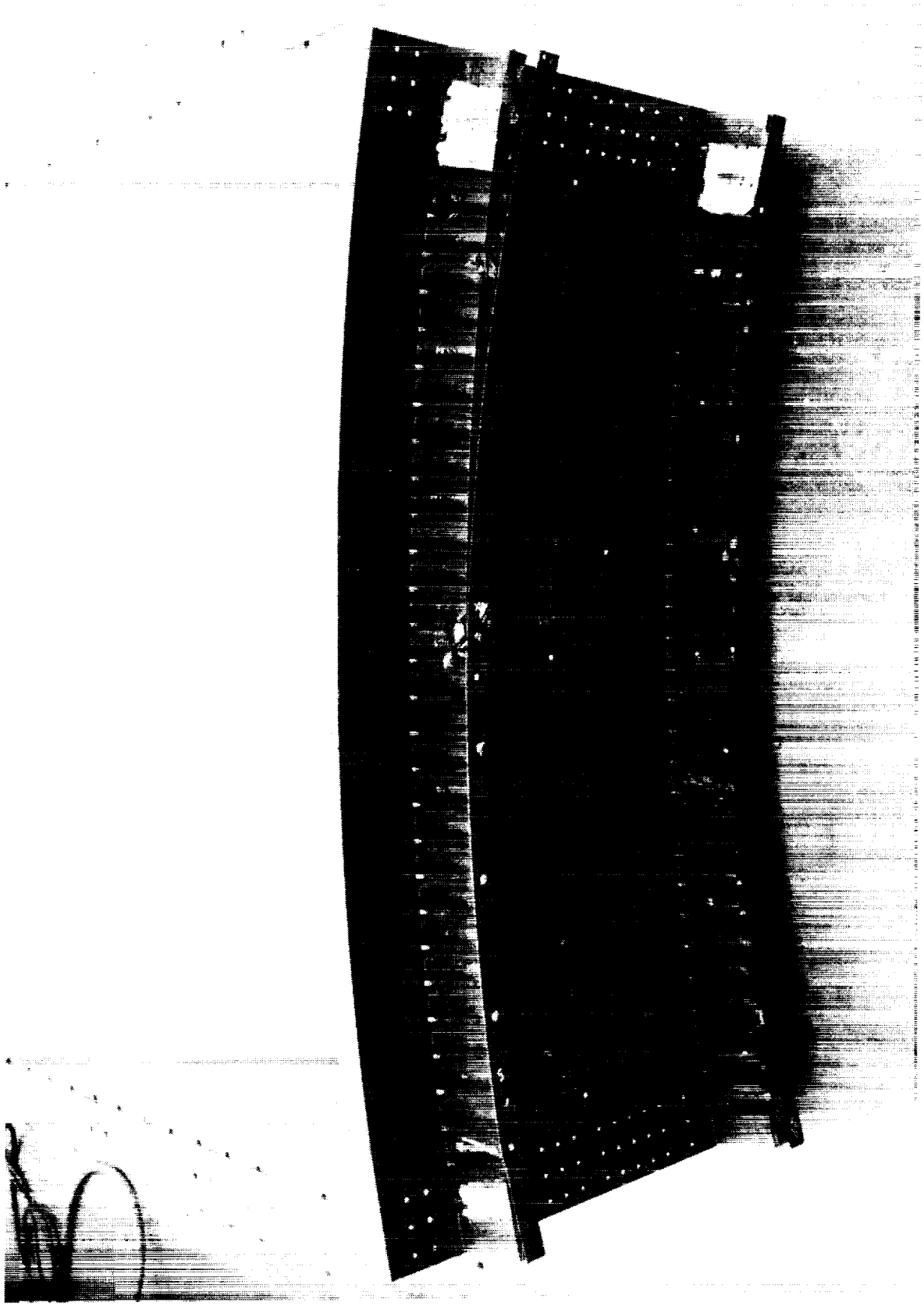

L-89-4473

(b) Frame/skin composite panel with damage.

Figure 15. Concluded.

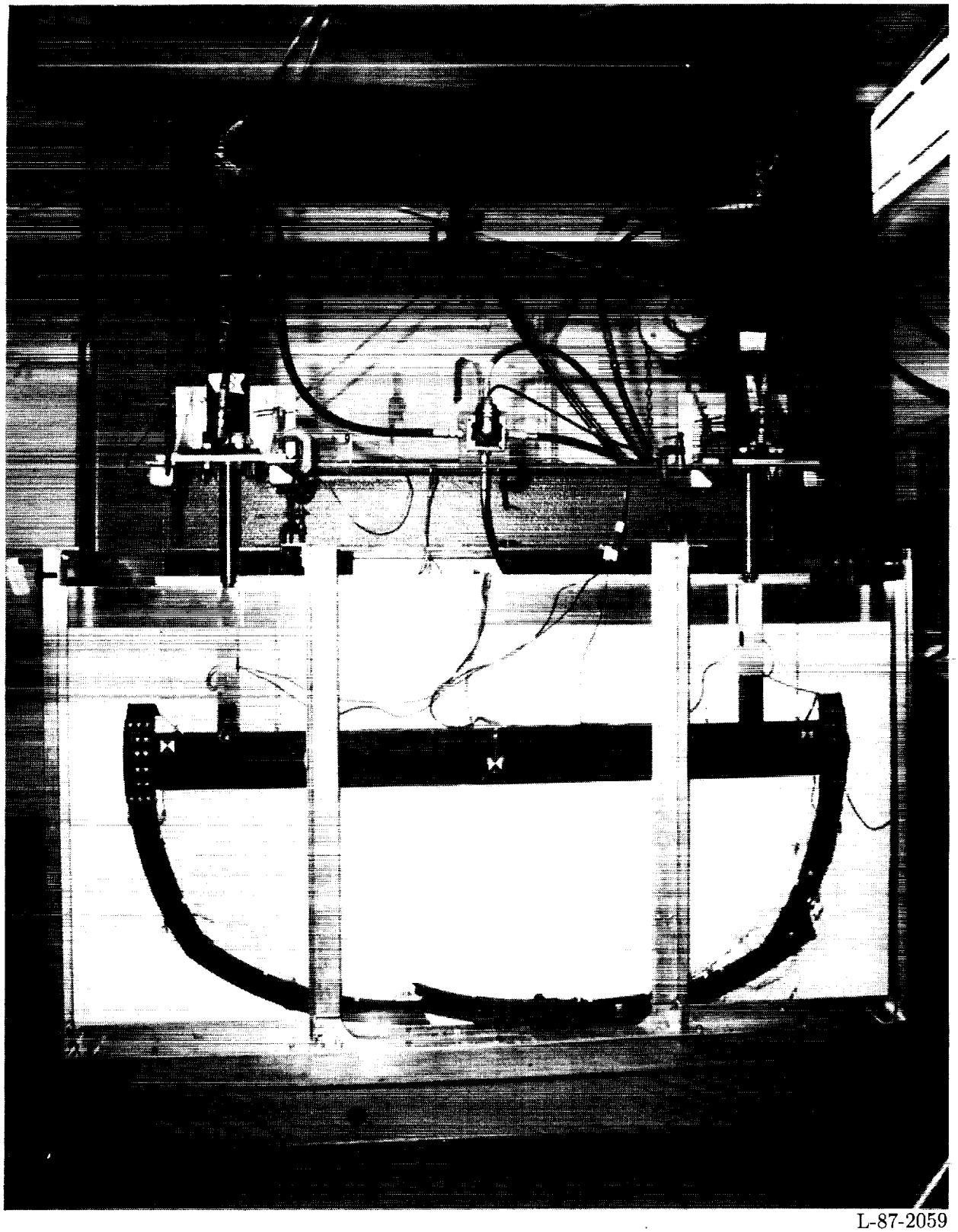

L-87-2059

(a) Static test apparatus.

Figure 16. Static results from tests of single composite Z-frame.

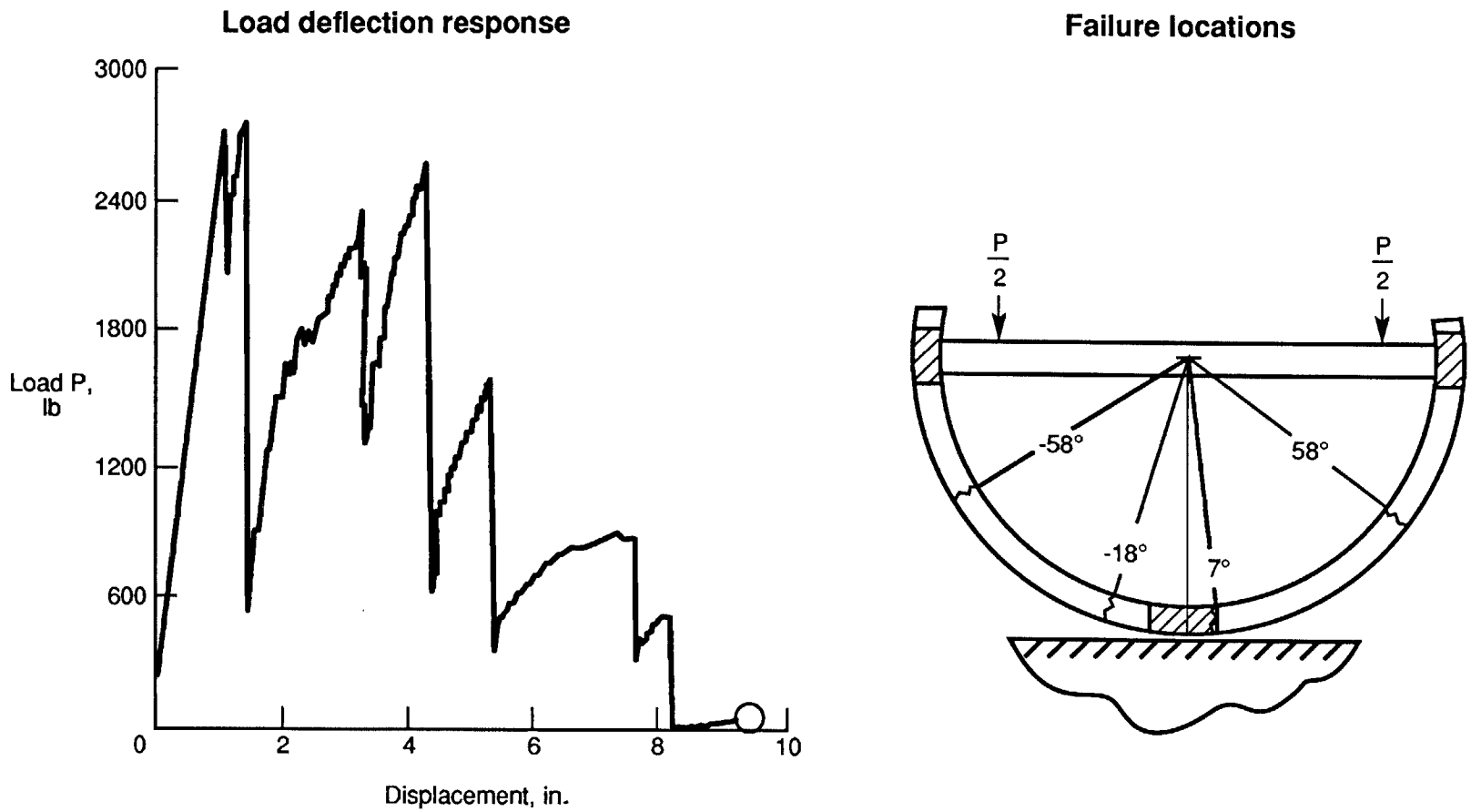

(b) Load displacement and failure locations.

Figure 16. Continued.

ORIGINAL PAGE
BLACK AND WHITE PHOTOGRAPH

Frame before cross-sectional failure

$t = t_1$

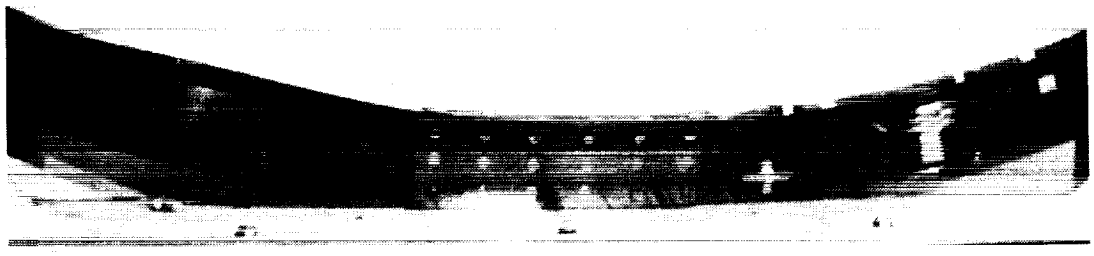

Frame after cross-sectional failure

$t = t_1 + 0.1$ sec

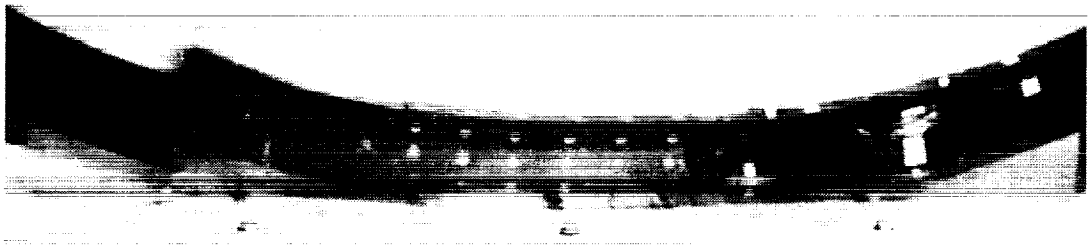

L-89-11843

(c) Frame local instability.

Figure 16. Concluded.

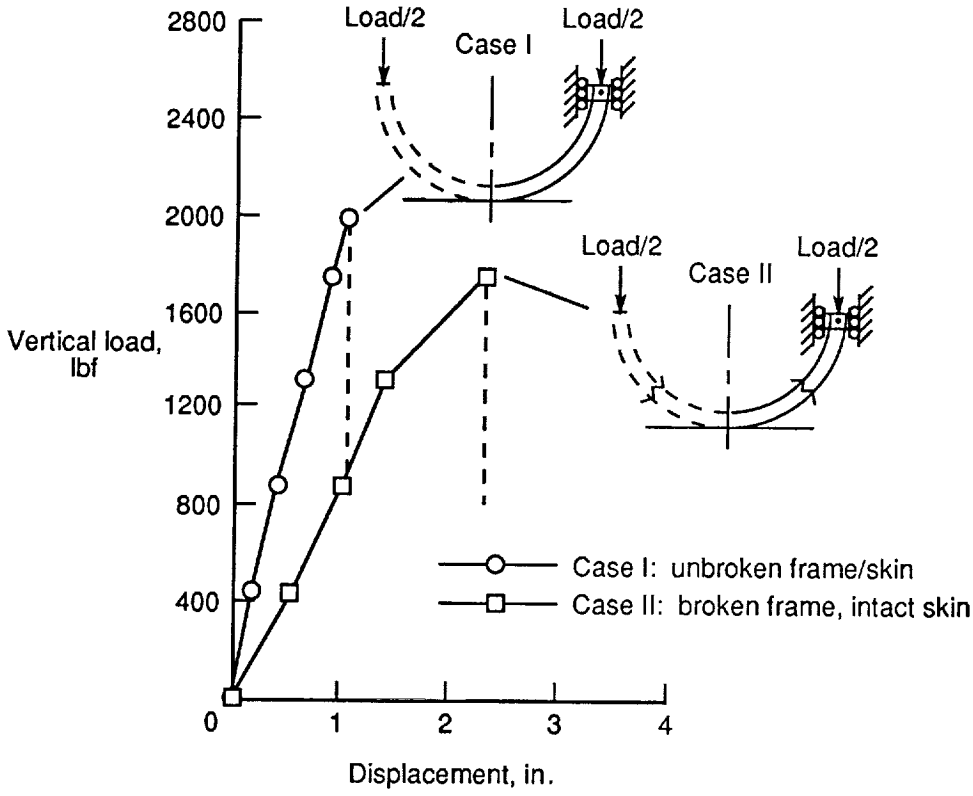

(a) Load displacement.

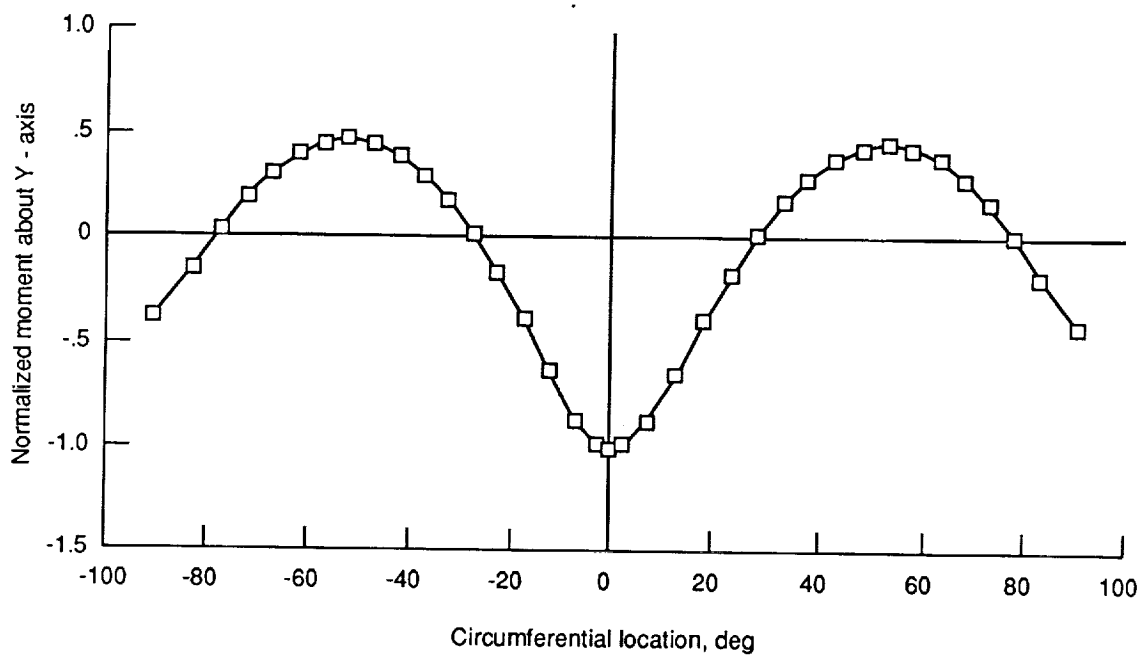

(b) Normalized moment (prior to initial break). Case I.

Figure 17. Typical analytical results for composite skinned frame using I-section frame for ease of analysis.

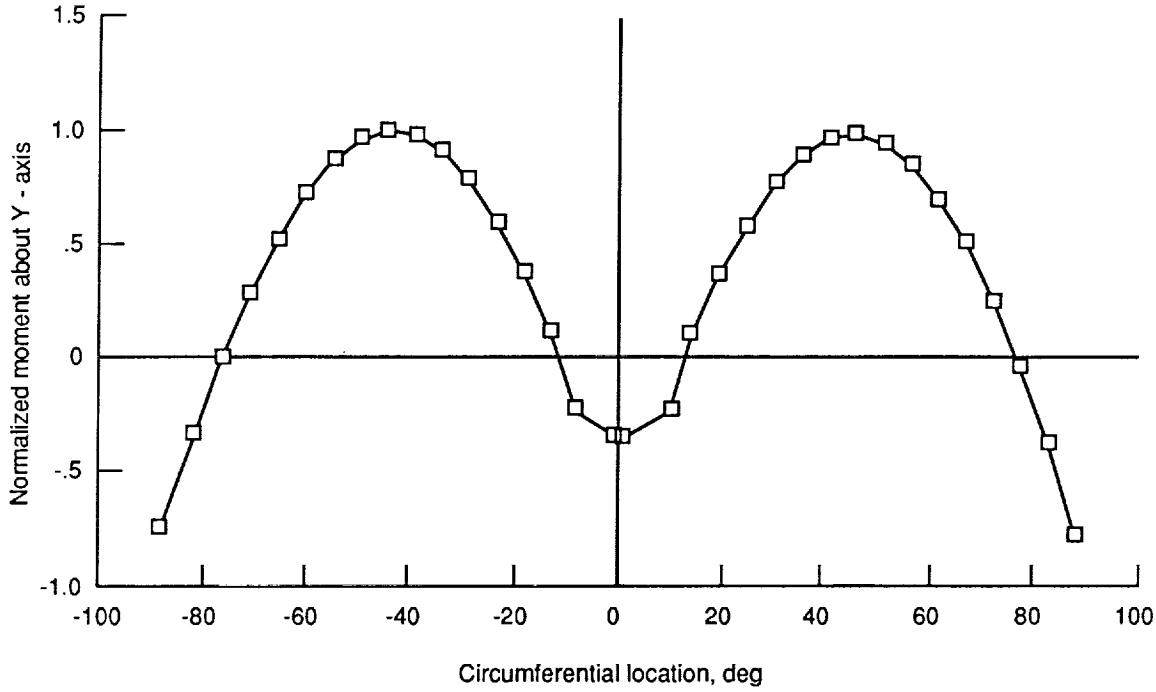

(c) Normalized moment (broken frame, intact skin). Case II.

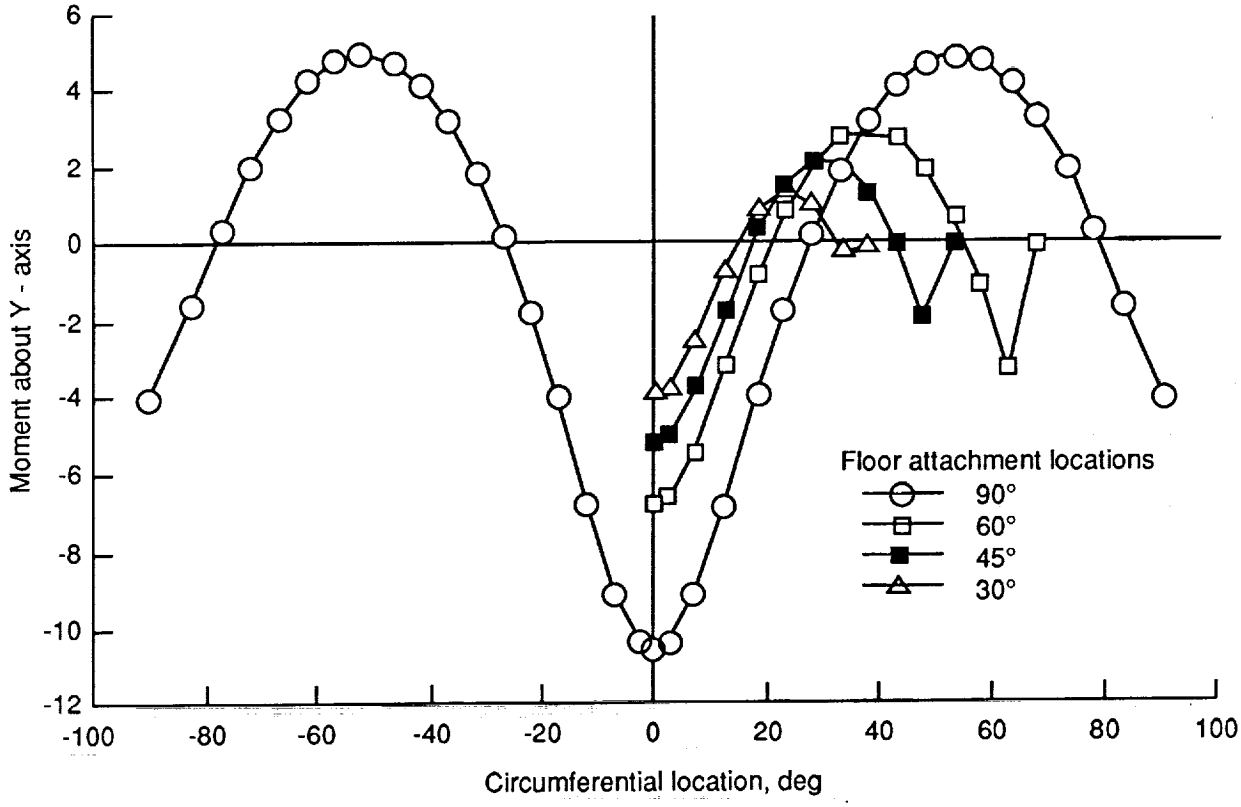

(d) Moment distribution (showing floor location effects).

Figure 17. Concluded.

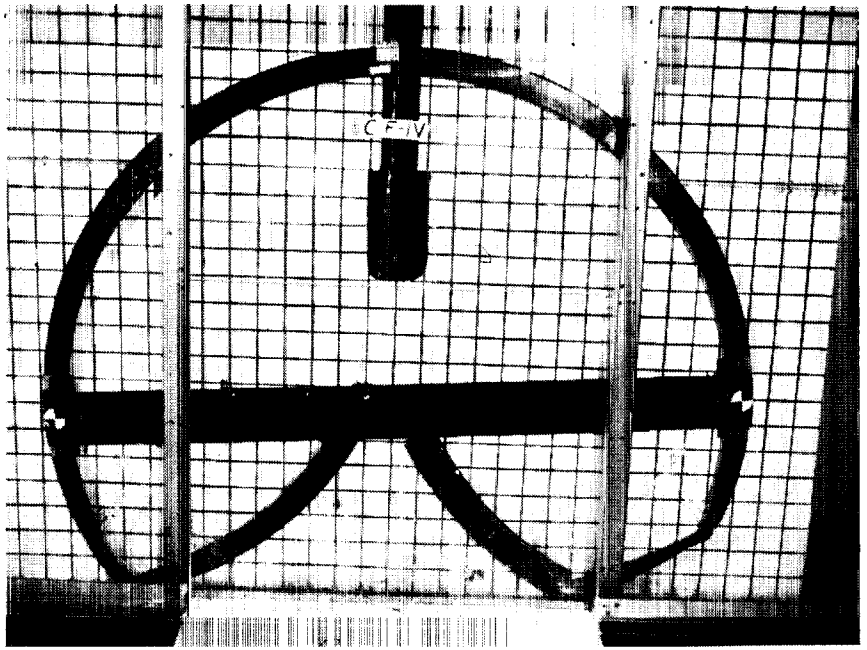

L-86-3528

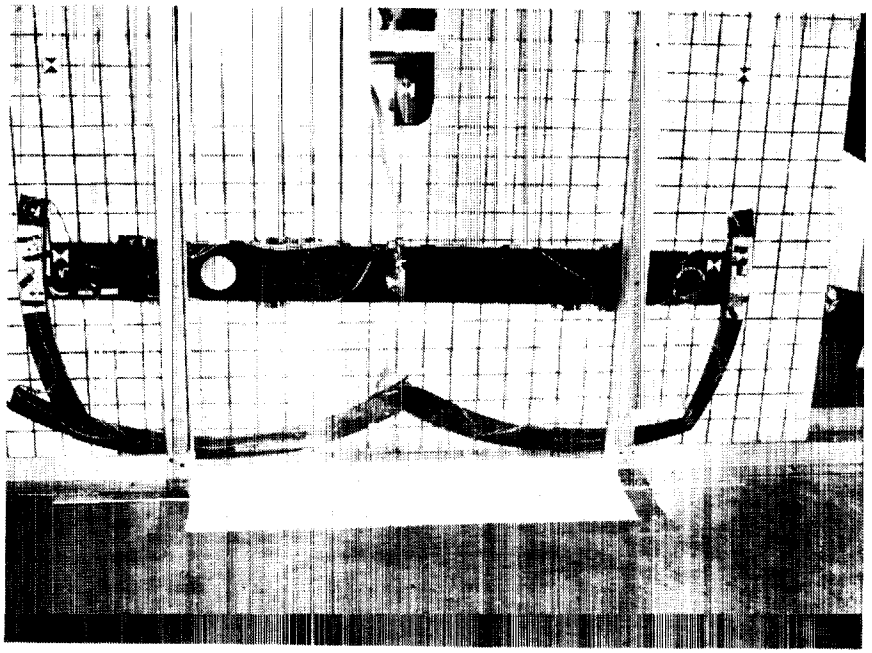

L-86-3234

(a) Photographs of failed frames.

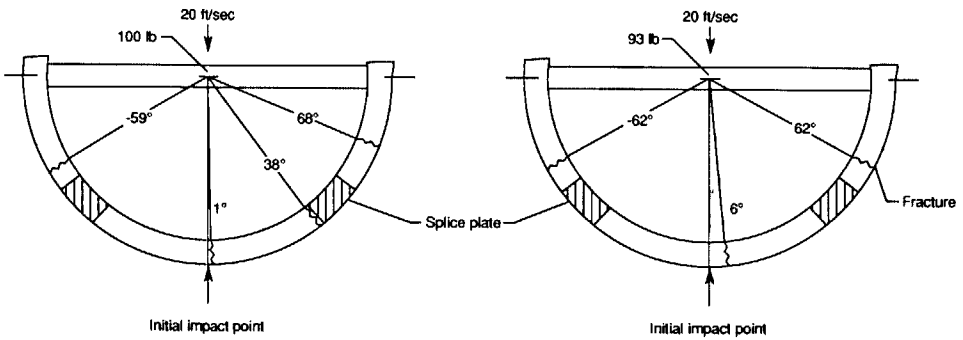

(b) Location of failures on frames.

Figure 18. Behavior of composite Z-frames under dynamic loading.

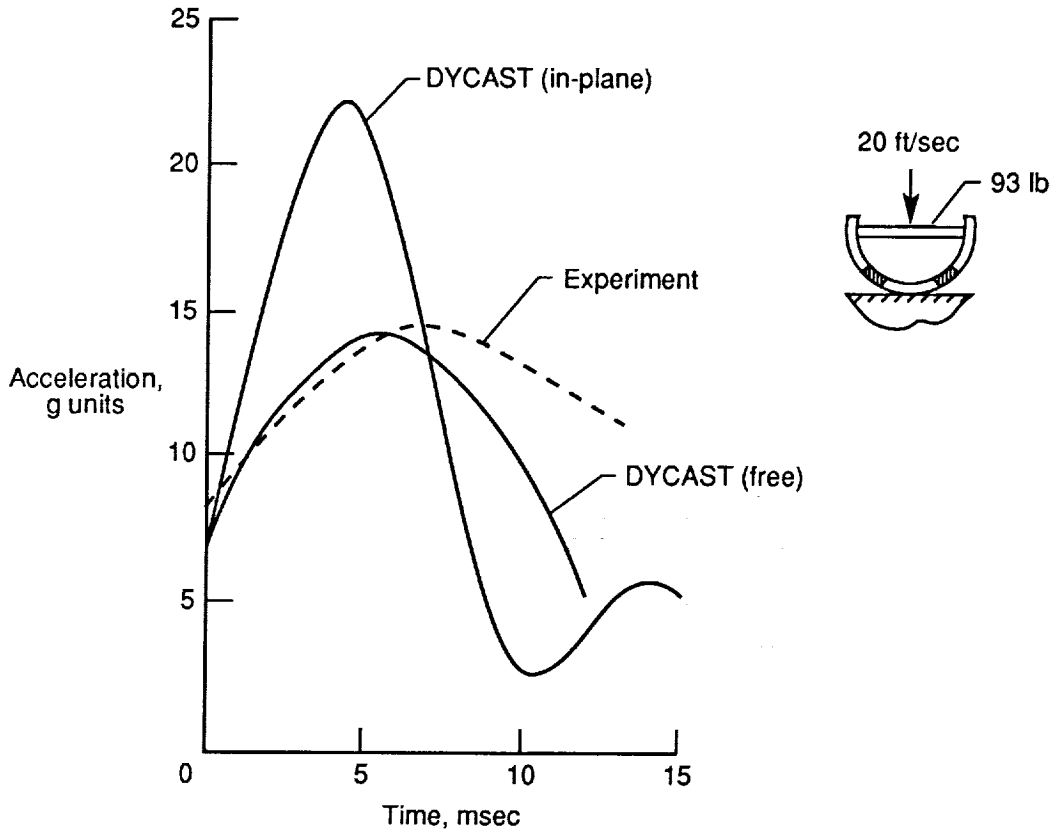

Figure 19. Comparison of experimental and analytical composite Z-frame accelerations.

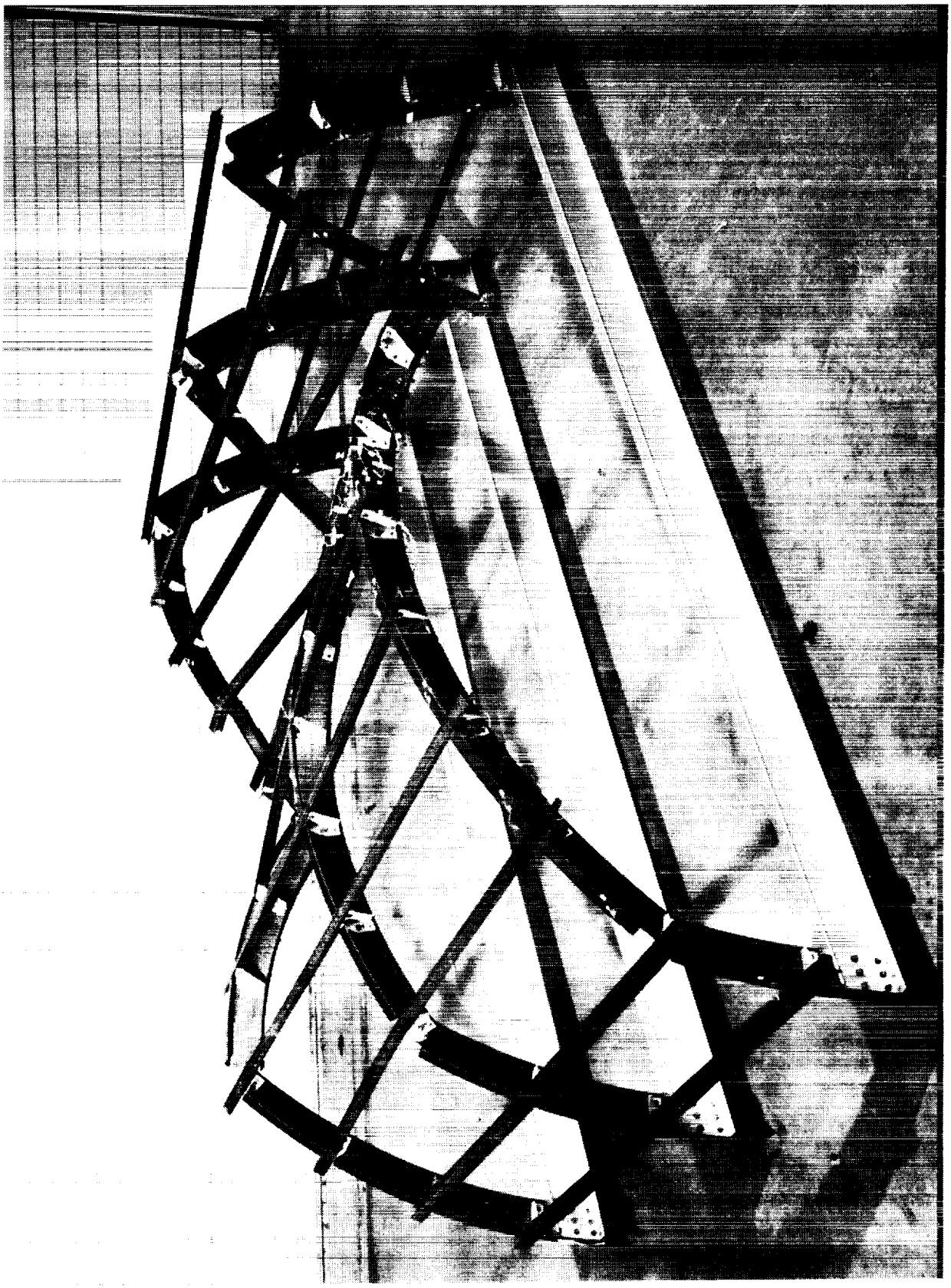

L-88-2459

(a) Failed skeleton subfloor after static test.

Figure 20. Behavior of composite skeleton subfloor under static loading tests.

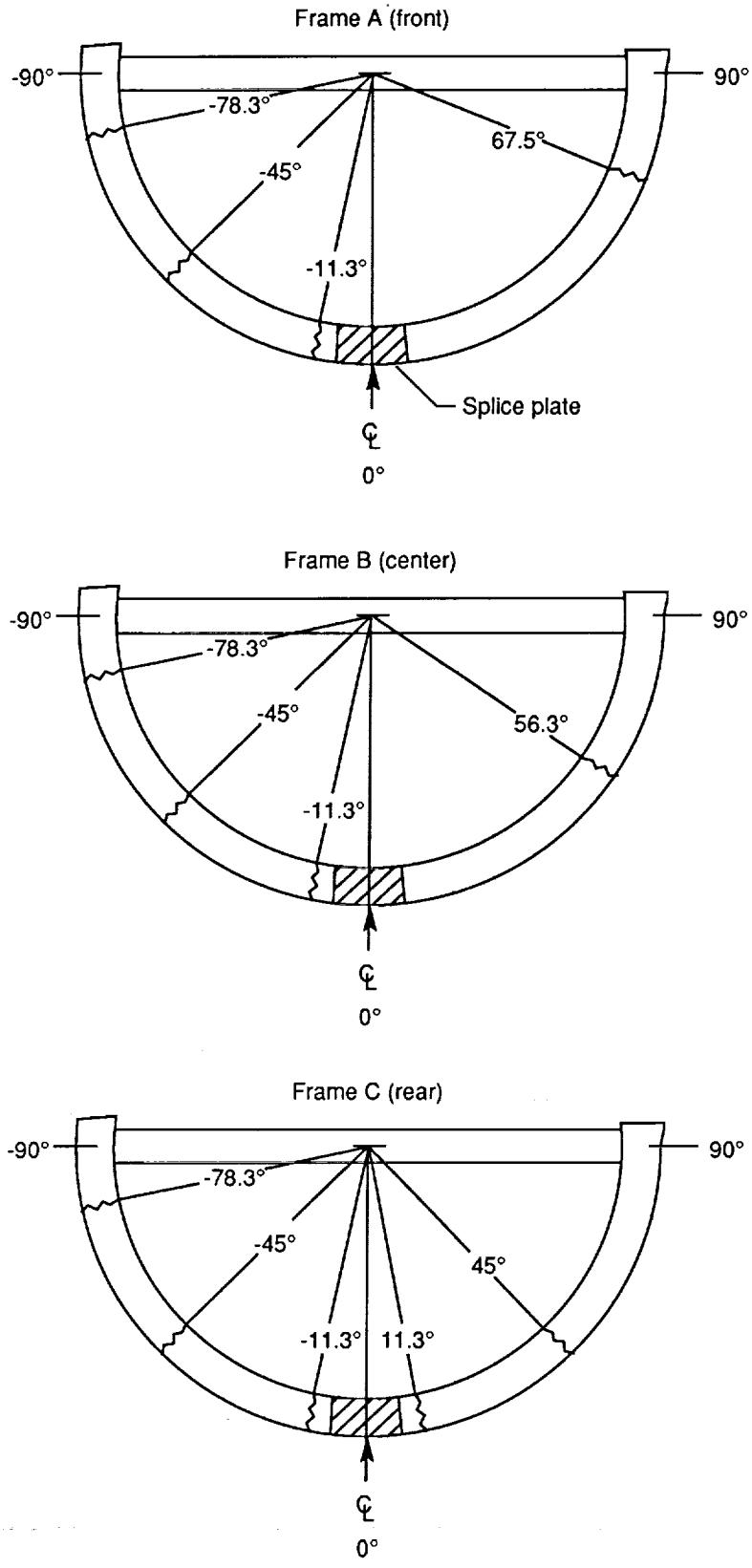

(b) Failure locations.

Figure 20. Concluded.

L-88-6710

(a) Failed skeleton subfloor after dynamic test.

Figure 21. Behavior of composite skeleton subfloor under dynamic loading tests.

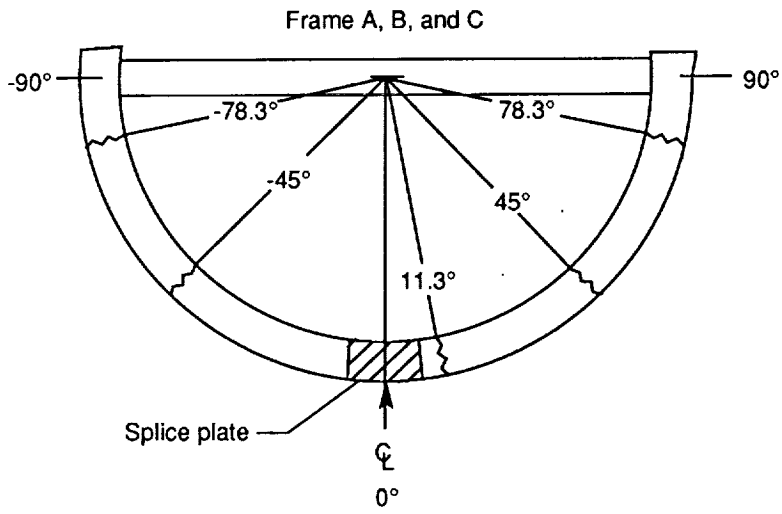

(b) Locations of failures.

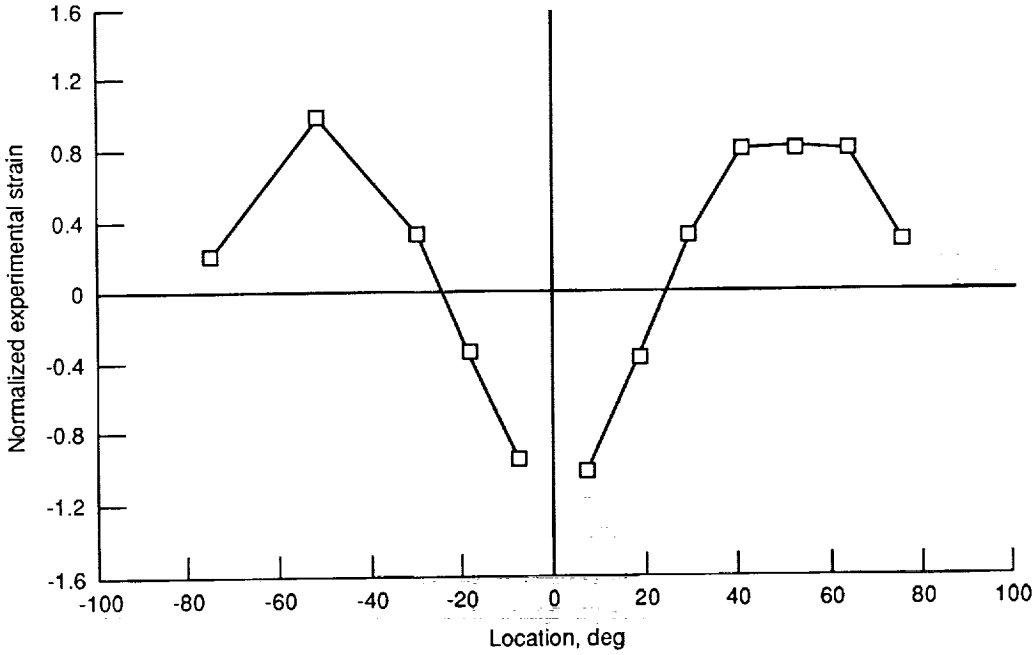

(c) Normalized circumferential strain distribution. Frame A.

Figure 21. Concluded.

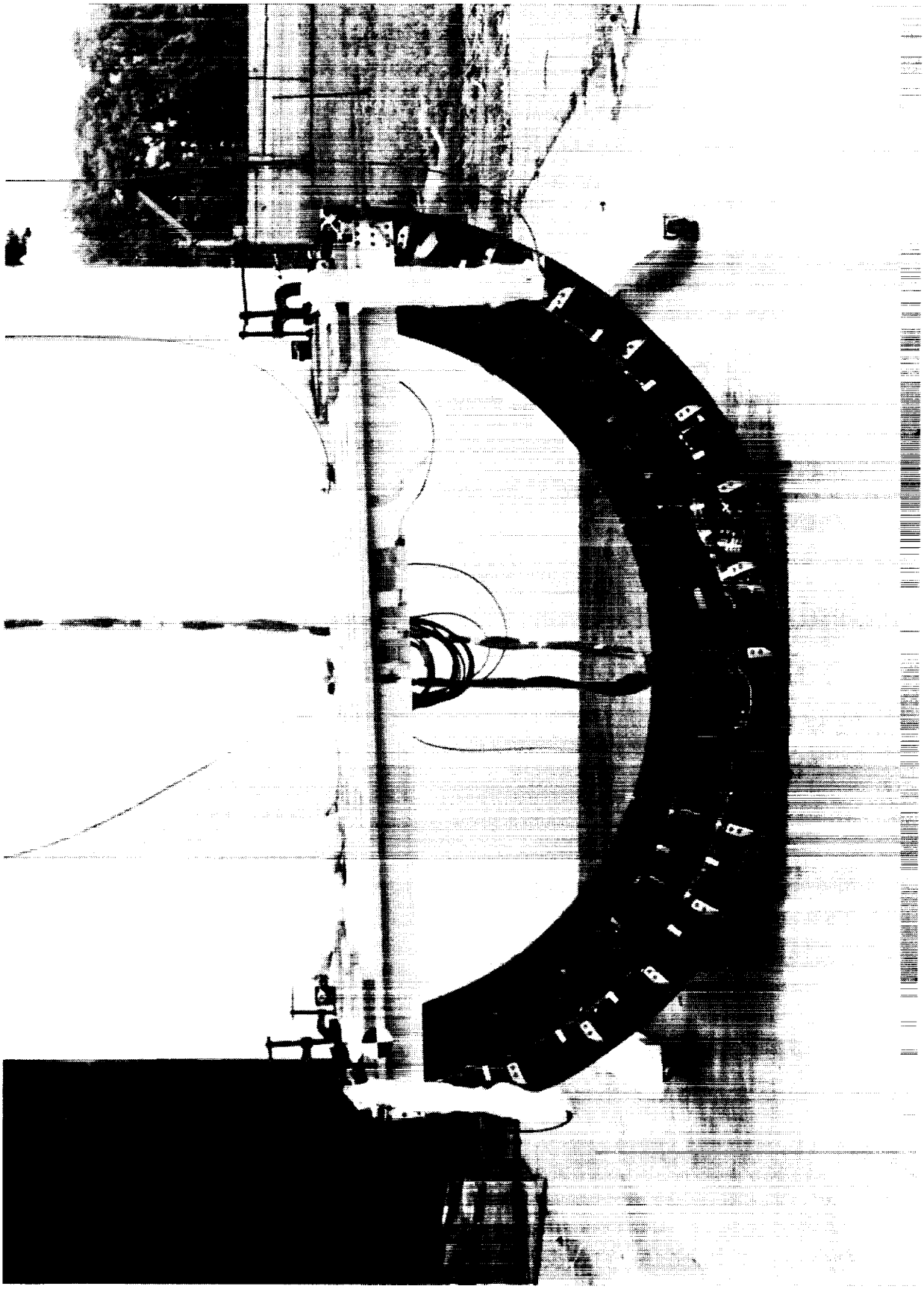

L-88-7589

(a) Failed skinned subfloor after drop test.

Figure 22. Behavior of skinned subfloor under dynamic loading tests.

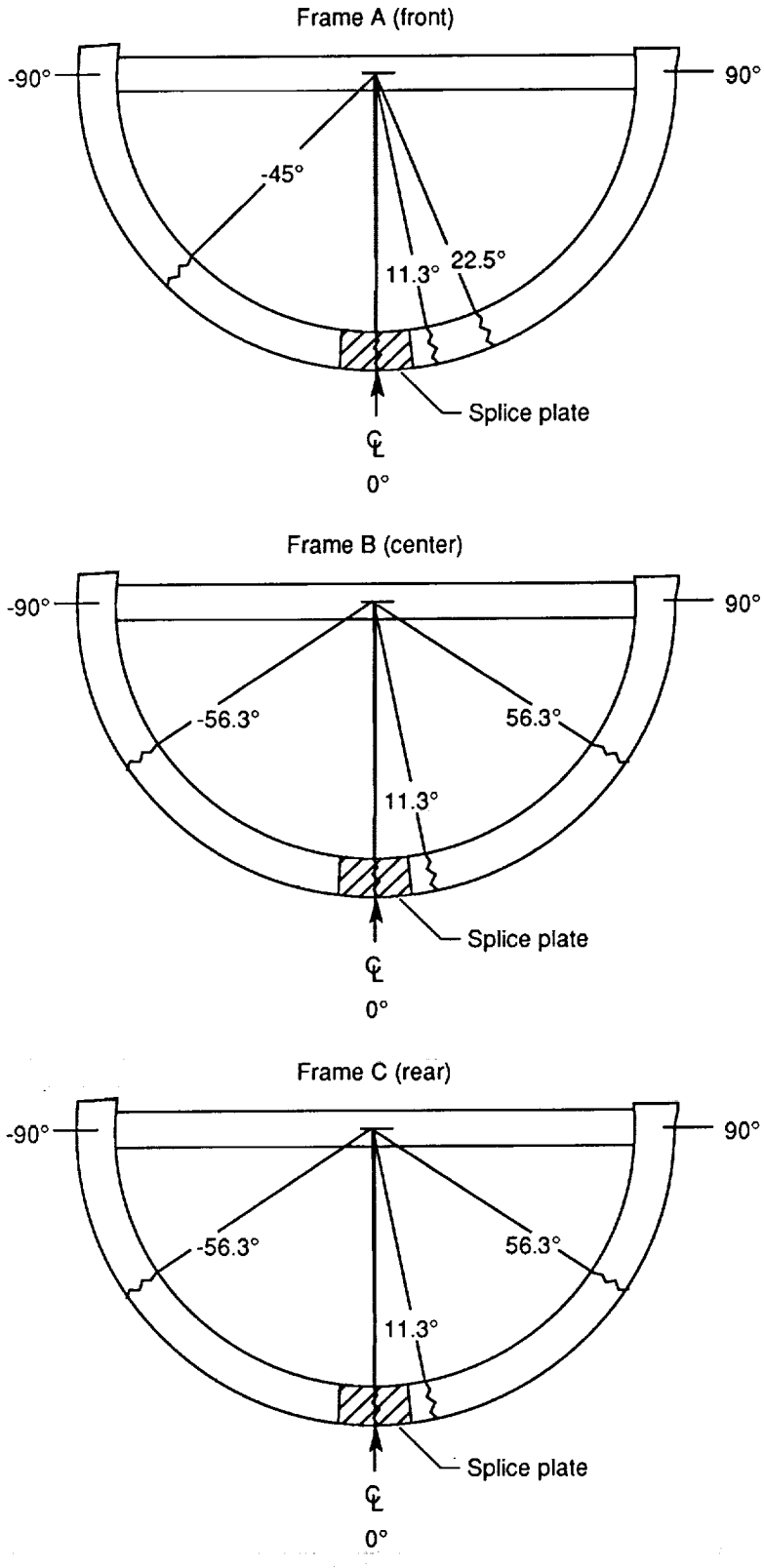

(b) Location of failures.

Figure 22. Continued.

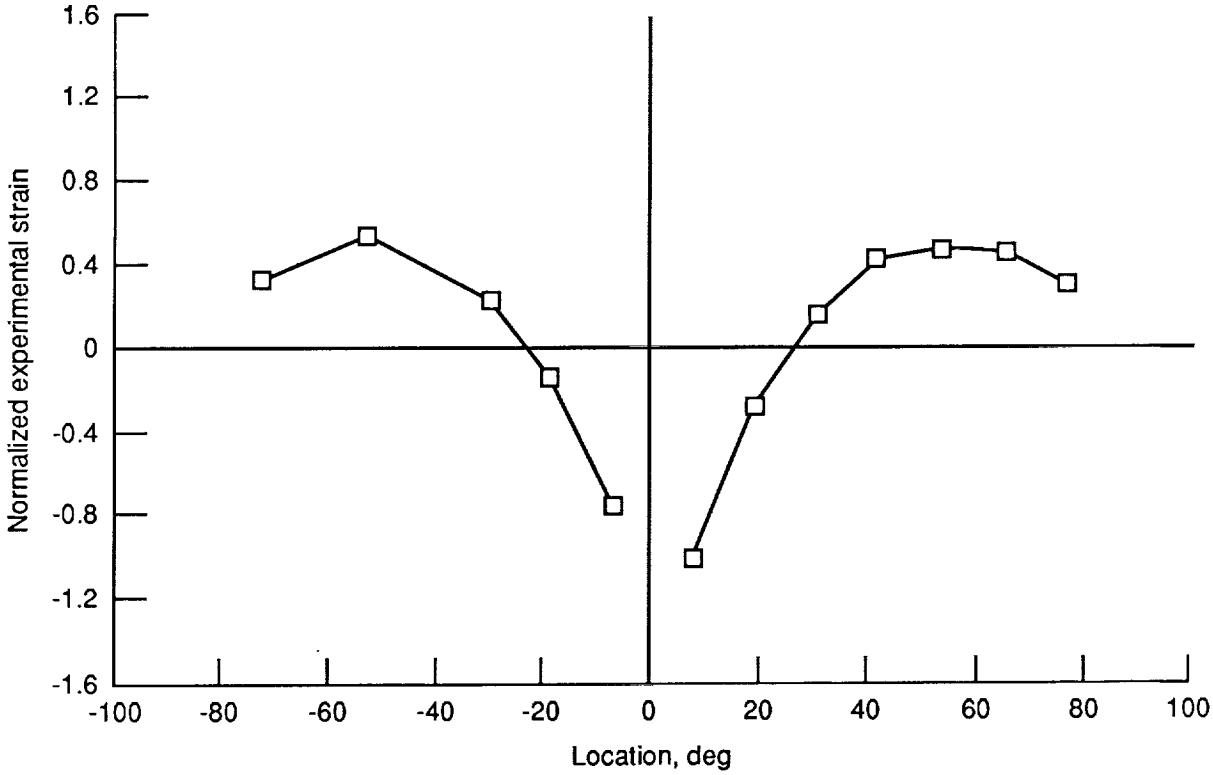

(c) Normalized circumferential strain distribution. Frame A.

Figure 22. Concluded.

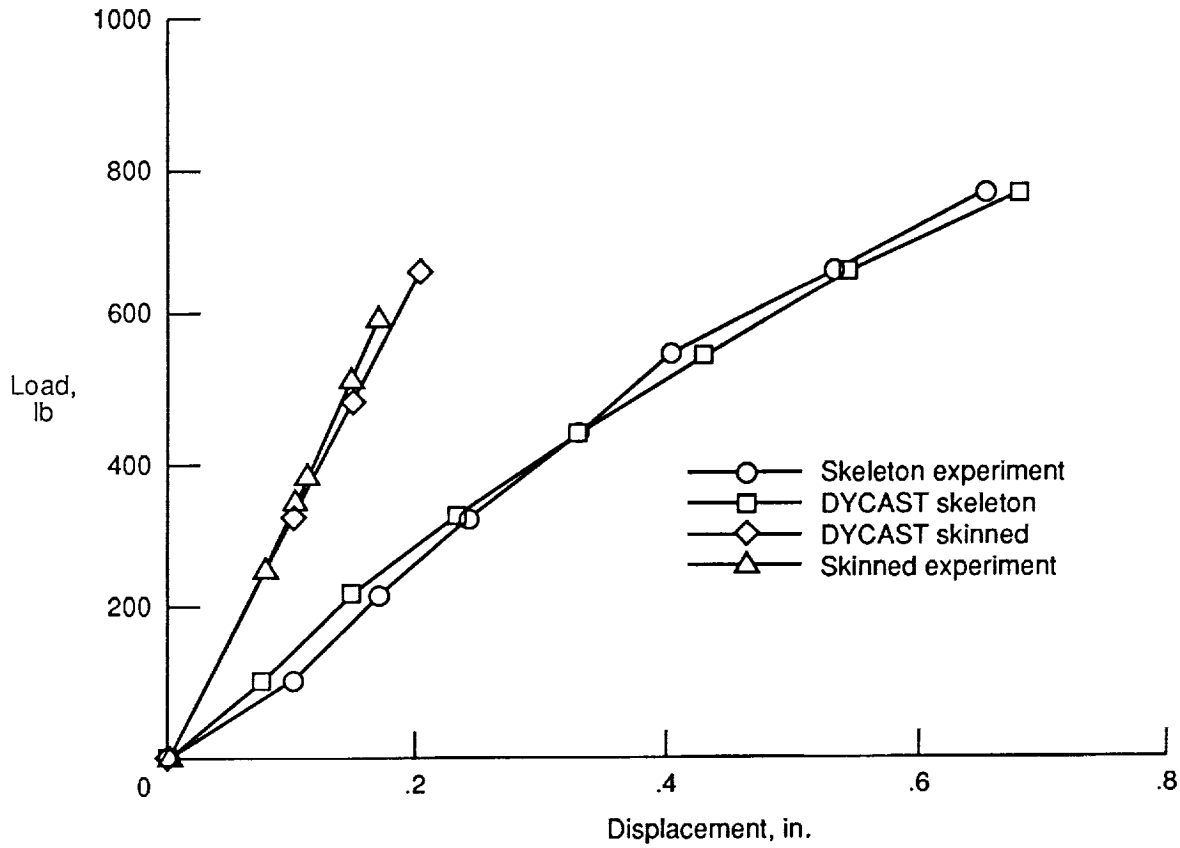

Figure 23. Comparison of experimental and analytical stiffnesses of skeleton and skinned composite subfloors.

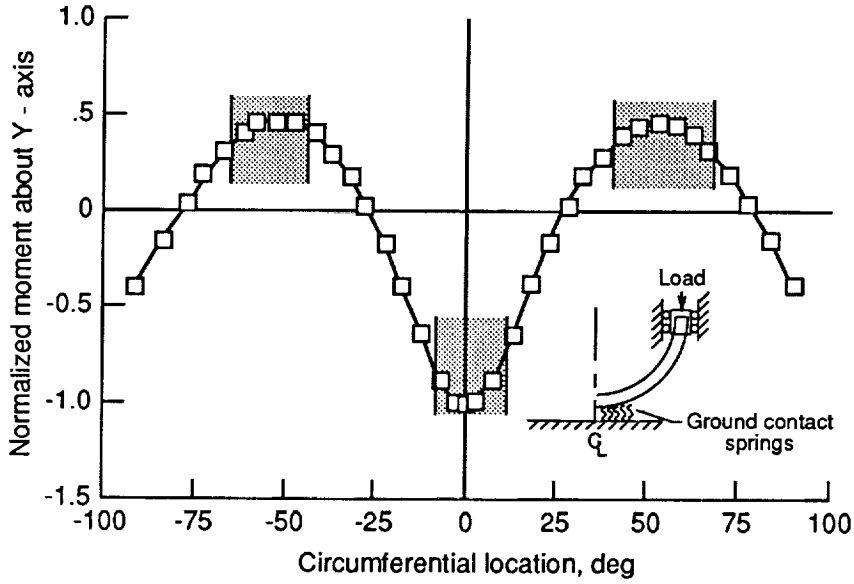

(a) Normalized moment distribution.

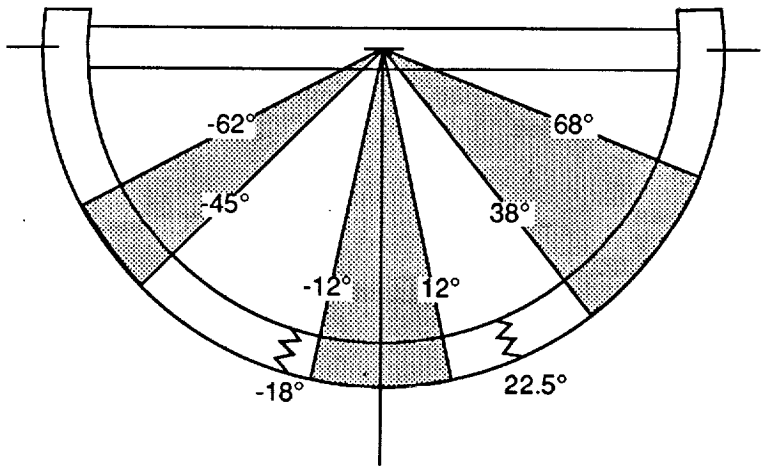

(b) Failure locations.

Figure 24. Comparison of nondimensional analytical moment distribution predicted by finite element frame model and observed failure locations (indicated by shaded regions) on metal and composite fuselage components and structures.

NASA
National Aeronautics and Space Administration

Report Documentation Page

1. Report No.	2. Government Accession No.	3. Recipient's Catalog No.
NASA RP-1239		

4. Title and Subtitle	5. Report Date
Failure Behavior of Generic Metallic and Composite Aircraft Structural Components Under Crash Loads	November 1990
	6. Performing Organization Code
7. Author(s)	8. Performing Organization Report No.
Huey D. Carden and Martha P. Robinson	L-16744
	10. Work Unit No.
9. Performing Organization Name and Address	505-63-01-11
NASA Langley Research Center Hampton, VA 23665-5225	11. Contract or Grant No.
	13. Type of Report and Period Covered
12. Sponsoring Agency Name and Address	Reference Publication
National Aeronautics and Space Administration Washington, DC 20546-0001	14. Sponsoring Agency Code

15. Supplementary Notes

16. Abstract

Failure behavior results are presented from crash dynamics research using concepts of aircraft elements and substructure not necessarily designed or optimized for energy absorption or crash loading considerations. To achieve desired new designs incorporating improved energy absorption capabilities often requires an understanding of how more conventional designs behave under crash loadings. The experimental and analytical data presented indicate some general trends in the failure behavior of a class of composite structures including individual fuselage frames, skeleton subfloors with stringers and floor beams without skin covering, and subfloors with skin added to the frame-stringer arrangement. Although the behavior is complex, a strong similarity in the static and dynamic failure behavior of these structures is illustrated through photographs of the experimental results and through analytical data of generic composite structural models.

17. Key Words (Suggested by Authors(s))
Crashworthiness
Composite structural response
Crash dynamics
Composite failure

18. Distribution Statement
Unclassified—Unlimited

Subject Category 39

19. Security Classif. (of this report)	20. Security Classif. (of this page)	21. No. of Pages	22. Price
Unclassified	Unclassified	46	A03

For sale by the National Technical Information Service, Springfield, Virginia 22161-2171